Structural Engineering

WELDED JOINTS FOR
TRIANGULAR TRUSSES

BY
R. G. REDWOOD AND P. J. HARRIS

JANUARY 1981
STRUCTURAL ENGINEERING SERIES No. 81-2

Department of Civil Engineering
and Applied Mechanics

McGill University
Montreal

WELDED JOINTS FOR TRIANGULAR TRUSSES

by

R. G. Redwood and P. J. Harris

C I D E C T

FINAL REPORT

PROJECT 5W

Structural Engineering Series No. 81-2

January 1981

McGill University

Department of Civil Engineering and Applied Mechanics

817 Sherbrooke Street West

Montreal, Quebec, Canada

H3A 2K6

ABSTRACT

This report describes ten tests of single panel segments of triangular trusses fabricated from RHS and hexagonal hollow sections. Attention was directed primarily at the behaviour of the joint where four web members are connected to the tension chord. Parameters investigated included the size of the gap, the ratio of web member width to chord width, the chord wall width to thickness ratio, the angle between web planes and the shape of the tension chord (square and hexagonal).

Observed failure modes included web member buckling, chord wall deformations at the joint and interaction between these two modes. Methods of analysis or design developed for planar truss joints may, in some cases, be applicable to triangular trusses. In general, the test results were found to lie within the range of the planar truss predictions. In other cases, planar truss analyses are not applicable, and methods especially developed for triangular trusses are needed.

* * * * * * * *

CONTENTS

1. INTRODUCTION

This report describes structural tests on ten segments of triangular trusses comprised of square and hexagonal tubular members. The objectives of this project were as follows:

> "to study the behaviour and develop appropriate design procedures for the web to bottom chord connections in trusses of triangular cross-section. In particular, the effect of two sets of web members in two different planes being attached to the bottom chord at the same point will be examined with a view to using present design methods for planar trusses in either their present or a modified form." (1)

This final report on the project provides a summary of all the work performed, and results are presented in sufficient detail to support the conclusions presented. Complete details are presented in two more detailed reports (2,3), and reference may also be made to two Progress Reports (4,5).

All test specimens comprised one panel of a Warren type triangular truss, as shown in Fig. 1, and represent a truss with one tension chord and two compression chords. While primary interest was focussed on the joint of the four web members to the tension chord, a truss panel was tested, rather than an isolated joint, in order to achieve realistic conditions in the web members framing into the joint of interest.

2. TEST SPECIMENS

2.1 Truss Specimens

The nominal dimensions of all truss segments are given in Fig. 1, and nominal member sizes are given in Table 1. With the exception of the tension chords of trusses 8, 9 and 10, all members were square HSS, provided by the Steel Company of Canada. The hexagonal members were provided by Tubes de la Providence, Lexy, France.

Actual values of the selected test parameters which influence the joint geometry and strength are given in Table 2. For specimens with square tension chords (nos. 1 to 7), the principal variables were the angle between web planes (90^0 and 60^0), the ratio of average web member width to chord width, β, the ratio of chord width to wall thickness, γ, and the magnitude of the joint gap. Specimens with hexagonal chords (Nos. 8 to 10) were essentially identical except for the size of the inclined web members.

For design purposes, the trusses were analysed as pin connected. The design of all the joints initially followed Ref. 6, which has been used in Canada since 1971 for the design of two-dimensional trusses. However, the designs of specimens nos. 6 to 10 were subsequently revised in an attempt to ensure joint failure in these later tests, since higher joint strengths were predicted by other design methods (7,8,9) and, in the first test series, several specimens showed relatively little joint distress. In order to obtain joint failure before the member failures, the following changes were made in specimens nos. 6 to 10:

(1) the thickness of the web members was increased to prevent them from buckling and yielding. (As a consequence of this, the new sizes ordered were not from the same heat of steel as that of the other members);

(2) the compression web members of specimens nos. 2 and 8 were

reinforced partway through the test in order to prevent buckling, and,

(3) the bottom chords of specimens nos. 9 and 10 were prestressed in compression to prevent yield in tension.

Measured dimensions of all members are given in Refs. 2 and 3, and were used in all calculations of member resistances and loads, etc. given in this report. In a number of cases, incorrect members were supplied, and in these cases nominal values for the supplied members are given in Table 1.

2.2 Material Properties and Fabrication

The specimens were fabricated from HSS members which were either hot formed to final shape or cold formed to final shape and stress relieved. For the square HSS, CSA G40.20 Class H and CSA G40.21 Grade 50W were specified. (The web members of specimen no. 7, however, appeared to be of CSA G40.21M Grade 480W.) For the hexagonal HSS, grade E-21 steel of the French standards was specified. The minimum specified properties for these material specifications are given in Table 3.

Three tensile test coupons were tested from each member meeting at the joint of interest, and were selected from tube walls other than the one containing the seam. Average results for these tests are given in Table 4 for each member.

The specimens were arc welded manually using low hydrogen electrodes of the E-480XX series (ultimate tensile strength = 480 MPa). Fillet welds were designed following Ref. 6, and the weld details at the joints under study are shown in Fig. 2. A reduced shop drawing of one specimen is shown in Fig. 3.

3. [illegible] METHOD

3.1 Test Arrangement

Nine of the specimens simulated the end panel of a simply supported truss in which the shear, and therefore the loads in the web members and on the joint, were maximum. One specimen (no. 3) simulated an interior panel in order to investigate the effect of having a higher average tension load in the chord.

The testing arrangement was chosen to simulate as closely as possible the conditions each panel would experience as part of a complete truss. Figs. 4, 5 and 6 show end panels in their inverted testing position. The specimen cantilevers from the rig, which is fixed to the strong floor, and is loaded by vertical loads at its end. These loads, applied through a loading beam with cables and hydraulic jacks under the strong floor, represent the shear at the support of the real truss. The internal reactions of the real truss at the imaginary cut between the end panel and the adjacent one and the means by which the rig provided them to the specimens were:

(a) tension only in the bottom chord, provided by the tendons,

(b) compression only in the top chords, provided by the horizontal rockers, and

(c) the internal transverse shear, provided by the vertical rockers.

In the case of Truss No. 3, a second reaction frame, identical to that shown in Fig. 4, was placed at the other end of the specimen, and the specimen was attached to it by tendons along the tension chord axis. No other connection was made to this second reaction frame, which thus served to apply uniform tension in the tension chord. Loading in shear took place in the same ways as for all other specimens. The small vertical component of the load applied by this rig, which resulted from deflections of the truss, was calculated and the applied shear load was corrected accordingly.

The reaction frames, tendons, and connections to the specimens were designed to resist, at ultimate, chord loads of 1780 kN, corresponding to a vertical load of 630 kN at the end of the truss segment.

In this report, the tension chord is referred to as the bottom chord, this being the usual position in a truss. It should be noted, however, that in the inverted test position this chord is in fact uppermost.

3.2 Instrumentation

Instrumentation comprised electric resistance strain gauges and mechanical deflection (dial) gauges. Details of the measurements taken and the quantities derived are given below.

3.2.1 Member Strains, Member Axial Forces and Bending Moments

Strain gauges were located at the third point sections of the bottom chord and of the compression and tension web members, and in addition some gauges were placed at the centres of the web compression members. Fig. 7 shows the locations of the sections on the members and Figs. 8 and 9 show typical locations of strain gauges at each of these sections on a specimen with square and hexagonal tension chords respectively.

The member axial forces and bending moments were obtained from these measured strains, and from the section dimensions and material properties, by summing the stress distributions round the sections.

These calculated member axial forces and bending moments are given in full in Refs. 2 and 3. Computer programs used for this data reduction are given in Ref. 3.

3.2.2 Measured and Corrected Joint Deformations Along the Axes of the Web Members

Joint deformations were measured parallel to the axes of the compression and tension web members relative to a plate tack welded normal to the adjacent unattached wall of the tension chord, as shown in Fig. 10.

Along each tension web member, one dial gauge measured directly the joint deformation. Along each compression web member, two dial gauges were used to measure both the deformation and the rotation due to the out of the web plane bending of the web member. By correcting for this rotation, the joint deformation along the web member centreline was calculated. Rotations due to the bending of the web members in the web planes were also measured with the dial gauges set perpendicularly to the web members. These rotations did not affect the measurements of the deformations along the axes of the web members, and since they are less important, they are not discussed further.

In the case of Trusses 1 to 5, only one deflection measurement was made parallel to the axis of the web compression member, and hence the resulting deflection overestimates the joint deformation along the axis, since it includes a component resulting from the rotation. Where comparisons are made in the following, between joint deformations of any of Trusses 1 to 5 with those of Trusses 6 to 10, the uncorrected values have therefore been used for the latter. The arrangement of dial gauges for Truss No. 7 is shown in Fig. 11(a).

In tests Nos. 1 to 7, this arrangement was satisfactory because the chord side walls bulged out very little, at least in the early stages of loading, and the plates stayed in position. In the first test of a hexagonal section, No. 10, the measurements became unreliable when the chord side walls deformed significantly out-of-plane and hence rotated the plates. In the later tests, (Nos. 8 and 9) therefore, because similar chord deformations were expected, the plates were supported away from the joint and extended to overhang it. This arrangement proved satisfactory and is shown in Fig. 11(b).

3.2.3 Shear Deformation of the Bottom Chord (Measured on Specimens Nos. 8 and 9 only)

The transverse deformation of the bottom chord on one side of the joint in relation to the other side was measured on specimens Nos. 8 and 9, with dial gauges placed transversely to one side of the chord and attached to a bar fixed on the other side of the chord. This arrangement is shown in Fig. 11(c). The recorded deformation was a measure of the shear deformation of the bottom chord at the joint but also reflected, to a lesser degree, some bending in the chord.

3.2.4 Mid-Length Transverse Deflections and Curvatures of the Compression Web Members

The transverse deflections were measured both in and out of the web planes by two dial gauges fixed to a bar supported at the ends of the compression web members. This arrangement is shown in Fig. 11(d). The transverse deflections and the curvatures obtained from the strains at the mid-length were used to detect the bending and the buckling of the compression web members both in and out of the planes of the webs.

3.2.5 Specimen Overall Measured Deformations and Corrected Truss Deflections

The overall deformations at the ends of the trusses were measured with dial gauges placed at each corner as shown in Fig. 1. The curves showing the transverse deflections of one end of the trusses relative to the other end were obtained by subtracting from the measured truss deformations the rigid body components due to the flexibility of the testing rig.

3.3 Loading

Loads were applied by means of hydraulic jacks, and at least ten loading steps were used in each test. Readings were taken at each loading step just after applying the loads. In test No. 3, the initial uniform tension applied by the second loading rig was maintained constant throughout the test. On the other hand, the prestressing loads in the tension chords of Trusses 9 and 10 were increased proportionately with the transverse shear. At each step, the shear load was applied first followed by the prestressing load and the readings were then taken.

4. ANALYSIS AND DESIGN ASPECTS

In this section, the bases for the calculated values of joint and member strengths are outlined.

4.1 Joint Strengths

In the absence of previous research work on joints in triangular trusses such as those considered herein, previous results used in design and research and developed for joints in planar trusses were examined. In the case of a 90^0 triangular truss with a square tension chord, the web members lie in a plane which is normal to the wall of the chord to which they are attached. The same is true of a 60^0 truss with an hexagonal chord. In these cases, if the joint resistance is determined by deformations of the chord wall to which the web members are attached, or by limiting behaviour in the web members, it is reasonable to expect some correlation between the planar and triangular truss joint behaviour. If, on the other hand, the joint resistance is governed by failure modes involving the unattached chord wall, the loss of symmetry about the web plane would preclude a close correlation. This lack of symmetry will also exist in the case of the 60^0 truss with a square tension chord. Of the ten test specimens, eight correspond to the conditions described above, which potentially could lead to similar behaviour of the planar and triangular truss joints, and this justifies an examination of planar truss joint strength predictions.

Seven of the ten specimens had RR-type joints (RHS web to RHS chord members) and the joint strength proposals examined for these were the Sheffield curve(10), the Corby curves(7), the Delft equation(11), and the computer program developed by Packer(8). Results obtained from these four methods are given for these seven test specimens in Tables 7 to 13.

The first three of these methods are concerned with joint behaviour only. On the other hand, the Packer program not only includes several modes of joint failure but also other associated modes of deformation and failure(8,20), and Tables 7 to 13 give loads at which four of these additional forms of behaviour are predicted. These are the following: joint deformation equal to 1% of the chord wall width; initial yield; and two local buckling mechanisms in the web compression member, one corresponding to axial compression in the member (M1) and the other corresponding to rotation of its end at the joint (M2).

Three specimens in the test program had RHex-type joints [RHS web to HexHS (Hexagonal Hollow Section) chord members], for which no design method was available. These cases were investigated by adapting joint strength proposals for both RR- and CC-Planar joints (CHS web to CHS chord members). The RR-planar joint strength methods used were the Sheffield curve, the Corby curves, and the Delft equation mentioned above. The CC-planar joint strength methods were the Stelco efficiency diagrams and the Delft equation for CC-joints.

Several assumptions were made in order to adapt these methods to the hexagonal section chords as follows: (a) to assume both circular and square chords with the same cross-sectional area and wall thickness as the hexagonal section, (b) to assume a circular section with the same wall thickness and with diameter equal to the distance between parallel walls of the hexagon and (c) to assume a square section with the same wall thickness and with walls equal in width to one wall of the hexagon. Results from these analyses are given in Tables 14 to 16.

4.2 Shear Strength of the Chord

The maximum shear stress in an HSS section occurs at the centroidal axis. By introducing an elastic shear constant, C_s, and using the von Mises yield criterion, the shear force on an HSS section, when the maximum shear stress reaches yield, is given by:

$$V_y = C_s \frac{\sigma_e}{\sqrt{3}} \qquad (4.1)$$

where C_s can be calculated by elementary theory.

The chord member in an HSS truss at a gap joint is subjected to the shear load from the vertical components of force in the web members. If, for simplicity, the effect of the axial load in the chord member is neglected, the shear resistance of the chord can be calculated using Eq. 4.1.

4.2.1 Planar Trusses

In planar trusses, the elastic shear stress distribution in an RHS chord is as shown in Fig. 12(a). The chord shear resistance corresponding to initial yield can be obtained from Eq. 2.1, where C_s has been given variously as:

from Stelco (12): $C_s = 2h_{0,flat} \cdot t_0$ (4.2)

where $h_{0,flat}$ is the flat portion of the chord side walls,

from Mouty (13): $C_s = 2h_0 \cdot t_0$ (4.3)

from Wardenier (9): $C_s = 2(h_0 + 2t_0) \cdot t_0$ (4.4)

4.2.2 Triangular Trusses

In triangular trusses, the elastic shear stress distributions in RHS and HexHS chord members are as shown in Fig. 12(b). The elastic shear constants are:

for an RHS chord member: $C_s \simeq 0.47\ A_0$, (4.5)

for an HexHS chord member: $C_s \simeq 0.48\ A_0$ (4.6)

The shear stress distribution in the chord member, when full yield is reached is shown in Fig. 12(c). The full yield shear resistance can be obtained from Eq. 4.1 using the following plastic shear constants:

for an RHS chord member: $C_{s,p} \simeq 0.71\ A_0$, (4.7)

for an HexHS chord member: $C_{s,p} \simeq 0.67\ A_0$ (4.8)

The ultimate shear resistance of RHS and HexHS chord members in triangular trusses may be expected to be bounded by the first yield and the full yield shear resistances.

In planar trusses with gap joints, the shear failure of the chord member generally becomes critical for values of $\beta = (b_1 + b_2)/2b_0$ greater than about 0.8. In triangular trusses, since the web members are usually smaller than in planar trusses because the shear is carried by two sets of web members, it can be expected that for gap joints the shear failure of the chord will become critical at lower values of β.

4.3 Truss Member Strengths

The strengths of the tension and compression members of the test trusses are discussed in subsequent sections in relation to the joint strengths.

Tension member strengths are calculated as the product of the cross-sectional area and the yield stress. In all cases, results are based on measured dimensions and measured material properties.

Compression member strengths have been evaluated by means of column strength curve No. 1 proposed by the Structural Stability Research Council (14.) This is the uppermost strength curve of three, and has been found to be applicable to HSS compression members of hot rolled or cold rolled, stress relieved material.

Compression web member strengths have been evaluated for several different effective length factors K, namely 0.7, 0.9 and the value based upon the method recently proposed in a CIDECT report (15).

5. TEST RESULTS AND DISCUSSION

The elastic behaviour of the trusses is described below in §5.1, and in §5.2 the individual truss behaviour at ultimate load is discussed in relation to the various observed failure modes. In §5.3, the influence of the main test parameters is discussed and compared.

5.1 Elastic Behaviour of Truss Specimens

Elastic analyses of the specimens were made with three different models, using the computer program SAP(23). These models assumed (a) pinned joints, (b) rigid joints with zero eccentricities and, for Trusses 6 to 10, (c) rigid joints with approximated eccentricities. Fig. 13 shows these three models for specimen No. 6. The member section properties were based on measured dimensions, and the nominal member lengths were used.

The analytical axial forces obtained from the three models agree within 3% in the worst case and within 1% in most cases. The experimental axial forces of all the specimens agree well with the analytical values. The experimental axial force is 82% of the analytical value (model 'a') in the worst case, 99% in the best case, and about 93% on average.

As expected, the analytical bending moments obtained from the three models differ considerably. The bending moments from model 'a' are zero, while those from model 'b' are different and smaller than those from model 'c'. Presumably, because of the inadequacies of the analytical models, the analytical bending moments correlate poorly with the experimental values.

Fig. 14 shows the axial force distribution in specimen No. 6 obtained from analysis 'a' together with experimental points. Fig. 15 shows the bending moment distribution obtained from 'c' together with experimental points.

The analytical overall deflections obtained from the three models agree within about 10%. The deflections obtained from models 'a' and 'b' are smaller than those from model 'c'. The experimental overall deflections of all the specimens agree well with the analytical values from the computer programs. For specimens 6 to 10, the experimental values were 80 to 104% of the predicted values using model 'c', as shown in Table 5.

5.2 Observed Modes of Failure

A summary of the test behaviour and the mode of failure of each individual truss is given in Table 6, and Tables 7 to 16 give, for each truss in turn, the predicted ultimate loads for each of the failure modes discussed in §4, together with the maximum experimental load. In the following comparisons with the predicted values, it should be recalled that the predicted values are based on planar truss joints and thus do not consider the presence of a second web plane. Complete descriptions of each individual test are given elsewhere (2,3), and in the following the results are described collectively according to the observed primary mode of failure, and Table 17 gives a summary of the observations according to these modes. Each specimen after test is illustrated in Fig. 16 where the predominant deformations are shown. Truss No. 7 is not included since no significant deformations were observed in the test, and for Truss No. 3, the web member buckling shown was accompanied by significant chord wall deformations which are not visible.

5.2.1 Joint Failures

The curves of the chord wall deformations in the direction of the axis of the compression web member on the side where the deformations were largest are given in Fig. 17. In Tests No. 1, 8-2, 9, and 10, the chord walls show a sudden loss of stiffness along the compression web members and the ultimate resistance of the joint was considered to have been closely approached.

In Test No. 1, significant joint deformations occurred, and interacted with the buckling of the compression web members, and all the joint strength predictions seemed to be unconservative, as shown in Table 7. The Sheffield predicted joint strength was, however, only 2% higher than the maximum applied in the test, whereas the other three predicted values based on the Corby, Delft and Packer methods were 47%, 30% and 36% higher than the test value.

For Tests 8-2, 9 and 10, various "equivalent" sections were assumed, as described in §4.1, in an attempt to predict the hexagonal chord joint strength using planar truss strength predictions. These values are shown in Tables 14 to 16, but in view of the observed modes of failure, which involved in all cases a flattening of the chord cross-section under the combined action of the two compression web members, it is unlikely that the predicted values can have much meaning. Indeed, little consistency is evident from the results in Tables 14 to 16.

In Tests No. 3, 4 and 6, the loss of stiffness of the chord walls under the web members was gradual and the joint deformations interacted with the buckling of the compression web members. In each case, the joint stiffness in the direction of the compression web member remains positive when the ultimate load corresponding to web member buckling is reached.

In Tests No. 2-s, 5 and 7, the measured deformation of the chord walls along the axes of the web members was very small, and primary failure was not associated with the joint.

The application of planar truss joint predictions to triangular trusses is only appropriate if the connected walls of the chord are deforming independently of the unconnected walls. Of the trusses with significant joint deformations, this condition appeared to apply strictly only to Trusses Nos. 1 and 6, and application to the latter, being a 60^0 truss, also may be questioned. Trusses 3 and 4, in which out-of-plane deformations of the unconnected walls occurred, thus clearly indicating unsymmetric behaviour, may nevertheless be amenable to analysis by the planar truss methods. Of these methods, the Sheffield curve and the 1% deformation and yield values of Packer give consistently conservative results for these four specimens, with the exception of the 2% overestimate by the Sheffield curve for No. 1. The Delft equation appears to give the closest value on average, and the Corby value is quite high, especially for Truss No. 4.

The initiation of yielding in shear in the walls of the tension chord is predicted in a number of tests at loads considerably less than the maximum test loads. This initial yielding does not appear to have much significance on the joint behaviour. The predicted load to cause full shear yield in the gap is higher than the maximum test loads in all tests except Nos. 9 and 10 (both with hexagonal chords). For these trusses, the high shear stresses will have made more critical the severe conditions created by the chord tension combined with the bending of the walls of the cross-section resulting from the transverse forces from the web members.

5.2.2 Local and Overall Buckling of the Compression Web Members

Local buckling of the compression web members was observed in Tests No. 2-s and 3. In these tests, the maximum load applied to the web members was respectively, 10% and 22% higher than the local buckling resistance predicted by Packer's computer program. In the other tests, the Packer computer values indicated high local buckling resistance and, in these other tests, local buckling was not observed. For the test series therefore, the program predictions have been consistent with the observations.

Overall buckling of the compression web members was observed in the Tests Nos. 1, 2-s, 3, 4, 5, 6 and 8-1. In Tests No. 1 and 6, the calculated buckling resistance of the web members, based on curve 1 of Ref. 14, and using effective length factors of 0.77 and 0.79, based on Ref. 15, were respectively, 15% and 16% higher than the maximum loads applied to the web members. The actual effective length factors, back-calculated from the measured applied loads, were about 0.9. In Tests Nos. 3 and 5, the calculated buckling resistances with K = 0.94 and 0.77, based on Ref. 15, were respectively, 7% and 9% lower than the maximum loads applied to the web members. The actual back-calculated effective length factors were about 0.7 in both tests. In Test No. 2-s, the overall buckling of the stiffened web members was simultaneous with or was induced by their local buckling. Because of the reinforcing in this case, the calculated buckling strength of the web members was approximate, and the actual effective length factors were not back-calculated. In Tests No. 4 and 8-1, buckling of the web members, as indicated by transverse deflections and central curvatures, was approached but not reached. The calculated buckling resistances with K = 0.96 and 0.74, based on Ref. 15, were respectively 10% and 9% higher than the maximum loads applied to the web members.

In short, the calculation of the effective length factor, by applying the analysis of Ref. 15, was conservative in Tests Nos. 3 and 5, and probably also in Tests Nos. 4 and 8-1, but was unconservative in Tests Nos. 1 and 6. It should be noted that relevance of the analysis of Ref. 15 to the triangular truss web members is questionable. On the one hand, the joints to the compression chords were either at an angle to, or on the corner of, the chords and had vertical and horizontal web members framing into them. On the other hand, the joints to the tension chord consisted of two sets of web members and in the 60^0 trusses, the web members were connected off centre and at an angle to the bottom chord. All these conditions differ from those assumed in Ref. 15.

It should be noted that, in Tests 1, 3, 4 and 6, buckling of the compression web members occurred or was imminent after significant joint deformations had developed. In the case of Nos. 1 and 6, buckling occurred at a lower load than predicted.

5.2.3 Tensile Yield Failures

Failure in Test 8-2 occurred at a load corresponding to 103% of the load corresponding to calculated tension chord yield. In Test 5, the ultimate load corresponded to 98% of the load expected to produce tension web member yield.

5.3 Influence of Main Parameters

The seven trusses with RHS tension chords were designed to provide information which could be related to each of the four main parameters: the joint gap, the web to chord wall width ratio, β, the chord wall width to thickness ratio, b_0/t_0, and the angle between web planes, α. The comparison tests are listed in pairs in Table 18 together with nominal values of the main parameters. The three hexagonal chord trusses are also included. Comparison between Tables 18 and 2 shows that, in some cases, the fabricated trusses had joint gaps which differed considerably from the nominal values. This should be considered in comparing the behaviour of the various trusses in the following paragraphs.

5.3.1 Joint Gap

Tests No. 1 (g = 25 mm) and No. 2 (g = 0 mm)

Gap joints, being generally weaker than lap joints, were studied in all ten specimens. The Sheffield, Corby and Delft design proposals do not take the magnitude of the gap into account in predicting the strength of a gap joint. However, it is generally recognized that a joint with a small gap is stronger than one with a large gap. Specimens No. 1 and 2 were nominally identical except for their gap sizes.

Due to the slightly higher yield strength of the tension chord of Truss No. 2, the Sheffield, Corby and Delft methods predict the ultimate strength of joint no. 2 to be about 5% greater than Truss No. 1, whereas the maximum test load applied to joint no. 2 was 124% of that applied to joint no. 1. The maximum load applied in Test No. 1 was associated with the interaction between the buckling of a compression web member and the joint deformations, whereas in Test No. 2 it was associated with the buckling of a compression web member without much joint deformation.

As can be seen from Fig. 17(a), showing the joint deformations, joint no. 2 was stiffer and deformed much less than joint no. 1, and this can be associated with the smaller gap size.

5.3.2 Relative Size of the Web and Chord Members

Because in triangular trusses the shear is divided between two webs, the web members are normally smaller than in planar trusses. For this reason, attention was directed to small ratios of web to chord member widths, expressed as $\beta = (b_1 + b_2)/2b_0$ which is of primary importance in all design recommendations. Values of $\beta = 0.4$ and 0.6 were considered in the three following cases.

(a) Tests No. 1 ($\beta = 0.4$) and No. 3 ($\beta = 0.6$)

According to the Sheffield, Corby, Delft and Packer proposals, the ultimate strength of joint no. 3 was predicted to be between 153% and 196% of that applied to joint no. 1, and the maximum test load applied on joint no. 3 was 229%. The maximum load applied in both tests was associated with the interaction between the buckling of a compression web member and the joint deformations. The difference in the resistances, and the stiffer behaviour of joint no. 3, can be seen in Fig. 17(b).

(b) Tests No. 5 ($\beta = 0.4$) and No. 7-2 ($\beta = 0.6$)

According to the Sheffield, Corby, Delft and Packer proposals, the ultimate strength of joint no. 7 was predicted to be between 153% and 216%

of that of joint no. 5, and the measured maximum load applied on joint no. 7 was 153% of that applied on joint no. 5. However, the maximum load applied in Test No. 5 was associated with the buckling of a compression web member, whereas in Test No. 7 the ultimate strength of the test specimen was not reached. Fig. 17(c) shows that the stiffer joint had the larger β value.

(c) Tests No. 6 (β = 0.4) and No. 4 (β = 0.6)

According to the Sheffield, Corby, Delft and Packer proposals, the ultimate strength of joint no. 4 was predicted to be respectively, 164%, 196%, 127% and 191% of that of joint no. 6. The measured maximum load applied on no. 4 was 113% of that applied on no. 6. The maximum load applied in both tests was associated with the interaction between the buckling of the compression web members and the joint deformations. As can be seen from Fig. 17(d), joint no. 4 was slightly stiffer than joint no. 6 and this behaviour can be associated with the higher β ratio of no. 4.

5.3.3 Chord Thickness

For planar truss gap joints, this is a very significant parameter and this was expected to apply also in the case of triangular trusses. Values of t_0 = 4.78 mm (b_0/t_0 = 26.6) and t_0 = 7.95 mm (b_0/t_0 = 16.0) were considered in the following cases:

(a) Tests No. 1 (t_0 = 4.78 mm) and No. 5 (t_0 = 7.95 mm)

According to the Sheffield, Corby, Delft and Packer proposals, the ultimate strength of joint no. 5 was predicted to be, respectively, 183%, 128%, 221% and 265% of that of joint no. 1, while the measured maximum load was 229%. The maximum load applied in Test No. 1 was associated with the interaction between the buckling of a compression web member and the joint deformations, whereas in Test No. 5 it was associated with the buckling of a compression web member without much joint deformation. Fig. 17(c) shows that joint no. 5, with the thicker chord walls, was stiffer and deformed much less than joint no. 1. Because of the lower stiffness of no. 1, the strength of the compression web member was decreased, the ratio of the experimental to predicted compression web member strength being about 10% lower in test no. 1 than in Test No. 5.

(b) Tests No. 3 (t_0 = 4.78 mm) and No. 7 (t_0 = 7.95 mm)

According to the Sheffield, Corby, Delft and Packer proposals, the ultimate strength of joint no. 7 was predicted to be, respectively, 173%, 139%, 260% and 294% of that of joint no. 3. The measured maximum load was 153%. The maximum load applied in Test No. 3 was associated with the interaction between the buckling of a compression web member and the joint deformations, whereas in Test No. 7 the ultimate strength was not reached. The deformations shown in Fig. 17(f) show the same trends as in Fig. 17(e).

5.3.4 Angle Between Web Planes, α

In trusses where this angle is 90^0, the joints are in some ways similar to those in planar trusses because the web members are connected at 90^0 to the chord walls. On the other hand, when α is 60^0, the web members are connected at 75^0 to the plane of the wall of a square chord. The angle between the web members and the chord, θ, was 45^0 in the 90^0 truss specimens and about 39^0 in the 60^0 trusses.

All comparisons between test specimens are expressed, in Fig. 17 for example, in terms of the shear in the truss, i.e. the test load applied at the end of the specimen. Because of the significantly different geometries of the 60^0 and 90^0 truss specimens, a given shear load in a truss leads to different forces on the joints in the two cases. Since the behaviour of a joint is normally dependent primarily on the load applied normal to the chord wall, the end shears on the trusses which are required to produce the same load normal to the chord walls in the 90^0 and 60^0 trusses have been computed. For unit compression force normal to the chord wall at the joint in the 90^0 truss, an end shear load of 1.41 is required, whereas the end shear would have to be 1.74 in the 60^0 truss, i.e. a 23% greater applied load. This should be considered when interpreting Figs. 17(g) and (h) and if these are used to compare deformations under identical normal loads on the chord walls, the 60^0 truss curve should be lower relative to the 90^0 truss results. It should also be noted that the compression web members in the 60^0 trusses were 9% shorter than those in the 90^0 trusses.

(a) Tests No. 1 ($\alpha = 90^0$) and No. 6 ($\alpha = 60^0$)

According to the Sheffield, Corby, Delft and Packer proposals, the shear load applied on truss no. 6 corresponding to the ultimate joint resistance was predicted to be, respectively, 120%, 121%, 141% and 160% of that applied on truss no. 1, while the measured maximum shear load applied on truss no. 6 was 198%, as shown in Fig. 17(g). The maximum applied shear loads in both tests were associated with the interaction between the buckling of a compression web member and the joint deformations. The 60^0 truss thus sustained a significantly higher normal load on its chord walls than the 90^0 truss.

(b) Tests No. 3 ($\alpha = 90^0$) and No. 4 ($\alpha = 60^0$)

According to the Sheffield, Corby, Delft and Packer proposals, the shear load applied on truss no. 4 corresponding to the ultimate joint resistance was predicted to be, respectively, 122%, 121%, 117% and 156% of that applied on truss no. 3, while the measured maximum shear load applied on truss no. 4 was 98%. The joint deformations are shown in Fig. 17(h). The maximum applied shear load was associated in both tests with the interaction between the compression web member buckling and the joint deformations, including deformations of the unattached chord walls. The ultimate load of truss no. 4 was not quite attained because the limit of travel of the specimen was reached.

In these two trusses, both with $\beta = 0.6$, the normal chord wall load sustained by the 60^0 truss was about 20% less than that sustained by the 90^0 truss. It is of interest to note that the reverse of this occurred in tests 1 and 6 for which β was 0.4. This suggests that because of the off centre attachment of the web members in the 60^0 trusses, as illustrated in Fig. 18, the joint strength in these trusses is less significantly influenced by low values of β than in a 90^0 truss. This is further illustrated by the comparison between the relative results for trusses 4 and 6 shown in Fig. 17(d) and the relative results for trusses 1 and 3 shown in Fig. 17(b).

5.3.5 RHex-Type Joints. Tests no. 8, 9 and 10

The three specimens, nos. 8, 9 and 10, were tested with three different web to chord member width ratios, $\beta = 0.51$, 0.68 and 0.85, respectively. Other joint parameters were identical. Joint deformation measurements are shown on Fig. 17(i).

The maximum applied test loads on trusses 8 and 9 were 75% and 85%, respectively, of that applied to truss 10, and joint stiffness also increased as β increased. The same trend is predicted by the Sheffield, Corby and Delft methods with the latter providing the more accurate indication of the strength variation. The mode of failure in all cases involved flattening of the chord section, with large lateral spreading and folding of the unattached side walls, as shown in Fig. 16(g) to (i). The punching into the chord of the web compression members was greater in trusses 8 and 9 than in 10, which had the larger β ratio. Consequently, in truss 10, the flattening of the chord section took place in the region of the gap, whereas in trusses 8 and 9 it occurred at the end of the web compression members and to some extent in the adjacent chord on the side away from the joint. The high shear stresses predicted by the analysis of §4.2.3 should also be noted, these being more critical in truss 10 than in 8.

6. PRINCIPAL OBSERVATIONS AND CONCLUSIONS

(i) In the test series, a variety of failure modes were observed. These included punching-in or push-pull failures of the tension chord walls, local and overall buckling of the compression web members, and an interaction of this buckling with joint deformations in some cases.

(ii) A triangular truss will carry one-half of the shear force in each web and, for all practical configurations, the force in each web will be less than in the web of an equivalent planar truss. Thus the web members of the triangular truss will, in general, be smaller than those of the equivalent planar one. In addition, for the same depth of truss, they will be longer. Thus, in general, it can be anticipated that the relative size of web member to tension chord member will be less than past experience with planar trusses would suggest. While this will generally lead to more severe conditions in the joint because of the smaller width ratio of the members, the capacities of the smaller and more slender web members are also more likely to be critical.

(iii) By assuming a column strength curve (curve 1 of [14]), effective length factors for those web members which underwent overall buckling were calculated. Values in the five relevant tests varied from 0.7 to 0.9. In two tests, the calculated K was equal to 0.9 (Tests 1 and 6) and in both cases significant chord wall deformations had taken place under the compression member ends prior to buckling. Other calculated K values were 0.74 or less.

(iv) Values of the effective length factors calculated using the proposed CIDECT method (15) were equal to or larger (i.e. conservative) than the values calculated from the test buckling loads, except for Tests 1 and 6, both of which exhibited significant chord wall deformations. However, the end conditions in the tests differed somewhat from those on which the results of (15) are based.

(v) In a 60^0 truss with a square tension chord with web members welded to adjacent sides, the off-centre attachment of the web members appears to diminish the sensitivity of the joint strength to a reduction in the parameter β, the ratio of web member width to chord width.

(vi) Hexagonal chords exhibited very large deformations at the joint, involving a flattening of the cross-section accompanied by outward displacements and folding of the chord side walls. Of the trusses with square section chords, only trusses 3 and 4 showed any significant flexure in the unconnected walls, and in these, the cross-sectional shape changed very little compared with those with hexagonal chords. The only direct comparison which can be made between 60^0 trusses with hexagonal and with rectangular sections is between trusses 9 and 6 respectively, since they had identical web members. Truss 6 sustained a load 15% greater than truss 9, but its chord area was 21% greater and chord wall thickness 6% greater. It appears, therefore, that there is no major difference in the joint strengths for rectangular and hexagonal chords of similar weight.

(vii) Member axial forces and deflections in the elastic range of loading may be calculated by treating the truss as a pin-jointed space truss. This applies to all types of joints and chords treated in the test series.

(viii) Measured moments in the elastic range were larger than those given by analysing the truss as a space frame, with assumed eccentricities in the joints.

(ix) The effect of the variation of the gap joint parameters in the triangular trusses showed the same trends as for the planar trusses:

- a joint with a small gap was found to be stiffer and stronger than one with a large gap;
- the joints with higher relative size of the web and chord members were found to be stiffer and stronger than those with lower values in 90^0 trusses;
- the joints with thicker chords were found to be stiffer and stronger than those with thinner chords.

(x) Previously developed methods of predicting the strength of planar truss joints might have some application to triangular truss joints. They will be particularly relevant to 90^0 trusses with square chords, when a punching type of failure involving only the connected chord wall is critical. There are considerable differences between current methods for planar trusses, which is partly due to their different bases (e.g. some are lower bounds to experimental results, others are based statistically on a given probability of not being exceeded, etc.). The limited number of test results for triangular trusses to which the planar truss methods might be applied, do not permit general conclusions to be reached. However, it may be noted that all results for trusses with rectangular chords lie within (or at most 2% outside) of the range of values given by the four methods considered.

(xi) Methods of analysis for triangular truss joints should be attempted in order to avoid the extensive and expensive testing which would be required of an empirical approach.

ACKNOWLEDGEMENT

Much of the work described in this report was carried out by two students working toward their Master of Engineering degrees: Martin Glebe, now of Marshall Steel Co., and Dominique Bauer, of McGill University. The writers wish to acknowledge these contributions and also that of their colleague, Dr. S. C. Shrivastava, who assisted in the design and verification of the test rig and specimens.

NOTATION

A_0	area of a section [mm^2]
b_0, b_1, b_2	width of RHS chord, compression web member, tension web member [mm]
B.C.	Bottom Chord
c1	column curve no. 1, Ref. (14)
C_s	elastic shear constant of a cross-section [mm^2]
$C_{s,p}$	plastic shear constant of a cross-section [mm^2]
CC-joint	a joint made of CHS web members connected to a CHS chord member
CHS	Circular Hollow Section
CR-joint	a joint made of CHS web members connected to an RHS chord member
C.W.M.	Compression Web Member
e	eccentricity of the joint [mm]
g	gap between toes of the web members [mm]
h_0, h_1, h_2	depth of RHS chord, compression web member, tension web member [mm]
HexHS	Hexagonal Hollow Section
HSS	Hollow Structural Section

K	effective length factor of a compression member
L	length of a member, measured from centreline to centreline [mm]
RHS	Rectangular Hollow Section
RHex-joint	a joint made of RHS web members connected to an HexHS chord member
RR-joint	a joint made of RHS web members connected to a RHS chord member
S1	side 1 of a triangular truss
S2	side 2 of a triangular truss
t_0, t_1, t_2	thickness of HSS chord, compression web member, tension web member [mm]
T.W.M.	Tension Web Member
V	total applied shear load on the specimens [kN]
V_y	shear on HSS to cause first yield [kN]
α	angle between the web planes in triangular trusses [deg]
β	mean width ratio between the web members and the chord = $(b_1 + b_2)/2b_0$ [mm]
θ_1	angle between the compression web member and the chord [deg]
θ_2	angle between the tension web member and the chord [deg]
σ_{e0}, σ_{e1}, σ_{e2}	yield stress of the chord, compression web members, tension web member [MPa]
σ_{ult}	ultimate stress [MPa]

REFERENCES

1. Triangular truss connections using HSS, Research Proposal to CIDECT, September 1976.

2. Glebe, M., Behaviour and strength of chord joints of triangular trusses made of hollow structural sections, McGill University, Structural Engineering Series, Report No. 80-2, September 1980.

3. Bauer, D., Tests of HSS triangular truss sections, McGill University, Structural Engineering Series No. 81-1, January 1981.

4. Progress Report on Welded joints in triangular trusses, CIDECT Project 5W, September 1979.

5. Progress Report No. 2 on Welded joints in triangular trusses, CIDECT Project 5W, April 1980.

6. Cran, J.A., Gibson, E.B., Stadnyckyj, S., "Hollow Structural Sections - Design Manual for Connections". Stelco, 1971.

7. British Steel Tubes Division, "RHS - Guide to Fabrication and Design".

8. Packer, J.A., "A Computer Program for the Structural Analysis of Welded Tubular Joints with RHS Chords". Advances in Engineering Software, 1979, Vol. 1, no. 4.

9. Wardenier, J., "Testing and Analysis of Truss Joints Made From Rectangular HSS", International Symposium on Hollow Structural Sections. Proceedings, Toronto, May 1977.

10. Eastwood, W., Wood, A.A., "Welded Joints in Tubular Structures Involving Rectangular Sections", Conference on Joints in Structures. University of Sheffield, England, September 1970.

11. Wardenier, J., Stark, J.W.B., "The Static Strength of Welded Lattice Girder Joints in Structural Hollow Sections". Part 4: Joints Made of Rectangular Hollow Sections. Stevin report no. 6-78-4, March 1978.

12. Gibson, E.G., Pastor, R.M., "Hollow Structural Sections - Design Manual for Columns and Beams", Stelco, 1973.

13. Mouty, J., "Theoretical Prediction of Welded Joint Strength". International Symposium on Hollow Structural Sections, Proceedings, Toronto, May 1977.

14. "Guide to Stability Design Criteria for Metal Structures", 3rd edition. B.G. Johnston, Editor, Wiley, 1976.

15. "Buckling Length of HSS Web Members Welded to HSS Chords". CIDECT Programmes 3E-3G (supplementary report - revised version). CIDECT Document 80/3-E, January 1980.

16. Dasgupta, A., "The Behaviour of Joints in Tubular Trusses". Thesis at the University of Nottingham, England, November 1970.

17. Davie and Giddings, T., "Research into the Strength of Welded Lattice Girder Joints in Structural Hollow Sections". University of Sheffield, England, CIDECT Programme 5EC, CIDECT Issue 71/7/E.

18. Richtlijnen Voor De Berekening Van Buisconstructies - Concept. "Regulations for the Calculation of Tubular Structures. RB 78". Delft, October 1977.

19. Packer, J.A. and Erdosy, L.,"A users guide to a computer program for the structural analysis of welded tubular joints with RHS chords". University of Toronto, Department of Civil Engineering, Publication No. 80-13, September 1980.

20. Packer, J.A., "Ultimate Load Analysis of RHS to RHS Gap Joints". CIDECT Interim Report no. CE 76/25 (5U), University of Nottingham, August 1976.

21. Bouwkamp, J.G., "Behaviour of Tubular Truss Joints Under Static Loads - Phase II", College of Engineering, University of California (Berkeley), Report no. 67-33, December 1967.

22. Washio, K., Togo, T., and Mitsui, Y., "Experimental Study on Local Failure of Chords in Tubular Truss Joints. Parts I and II", Technology reports of Osaka University, Vol. 18, no. 850 (1968) and Vol. 19, no. 874 (1969).

23. Gibson, E.G., Pastor, R.M., "Welded Joint Research Summaries - Hollow Structural Sections", Stelco, May 1974.

24. Wilson, E.L., Bath, K.J., and Peterson, E.E., "A Structural Analysis Program for Static and Dynamic Response of Linear Systems", University of California, 1974.

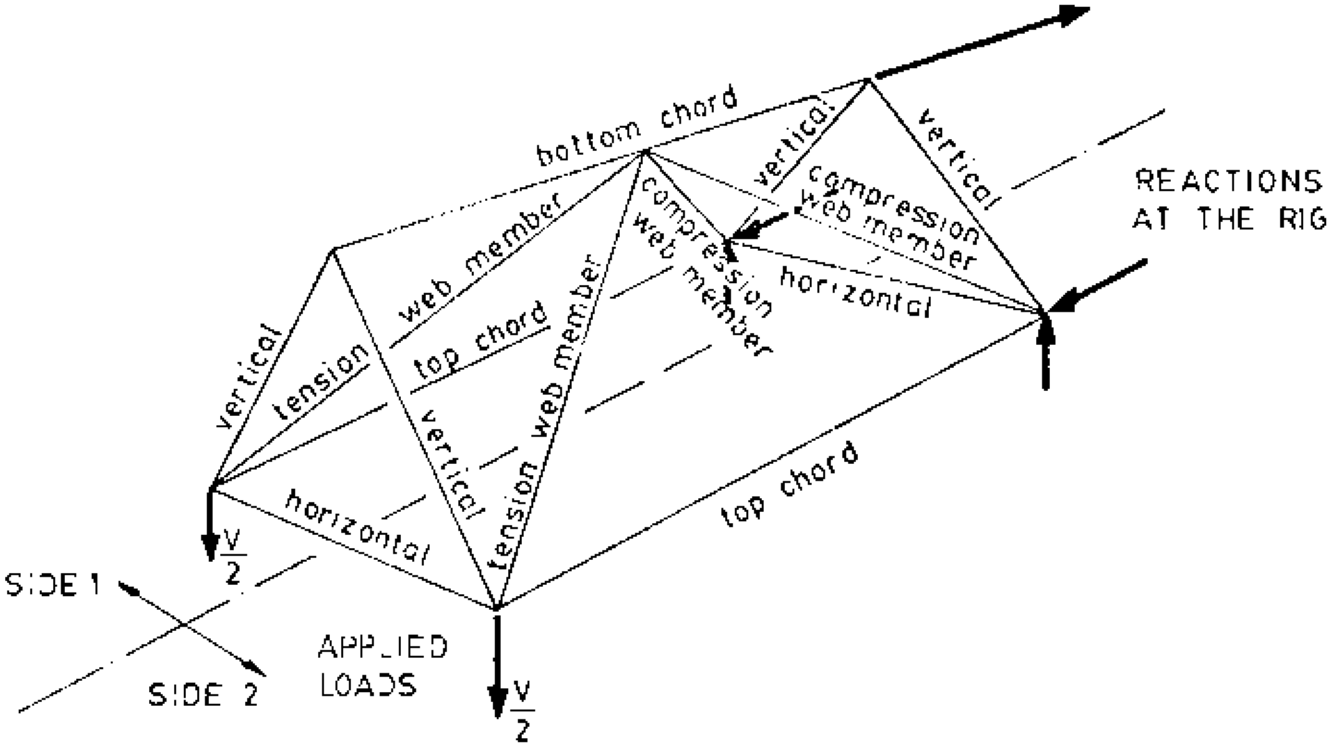

Truss no.	Members Framing at the Joint					Other Members		
	Bottom Chord	Compression Web Member on Side 1	Compression Web Member on Side 2	Tension Web Member on Side 1	Tension Web Member on Side 2	Top Chords	Verticals	Horizontals
1	127.0x127.0 x4.78	50.8x50.8 x2.79*	50.8x50.8 x3.81	50.8x50.8 x2.79	50.8x50.8 x3.81**	88.9x88.9 x4.78	50.8x50.8 x2.79	50.8x50.8 x2.79
2	127.0x127.0 x4.78	50.8x50.8 x2.79*	50.8x50.8 x2.79*	50.8x50.8 x2.79	50.8x50.8 x2.79	88.9x88.9 x4.78	50.8x50.8 x2.79	50.8x50.8 x2.79
2 R	"	" reinforced	" reinforced	"	"	"	"	"
3	127.0x127.0 x4.78	76.2x76.2 x3.81***	76.2x76.2 x3.18	76.2x76.2 x3.81***	76.2x76.2 x3.81***	88.9x88.9 x4.78	50.8x50.8 x2.79	50.8x50.8 x2.79
4	127.0x127.0 x4.78	76.2x76.2 x3.18	76.2x76.2 x3.18	76.2x76.2 x3.81***	76.2x76.2 x3.81***	88.9x88.9 x4.78	50.8x50.8 x2.79	50.8x50.8 x2.79
5	127.0x127.0 x7.95	50.8x50.8 x6.35	50.8x50.8 x6.35	50.8x50.8 x3.81	50.8x50.8 x3.81	88.9x88.9 x7.95	50.8x50.8 x2.79	50.8x50.8 x2.79
6	127.0x127.0 x4.78	50.8x50.8 x6.35	50.8x50.8 x6.35	50.8x50.8 x6.35	50.8x50.8 x4.78****	88.9x88.9 x7.95	50.8x50.8 x2.79	50.8x50.8 x2.79
7.1 7.2	127.0x127.0 x7.95	76.2x76.2 x7.95	76.2x76.2 x7.95	76.2x76.2 x7.95	76.2x76.2 x7.95	88.9x88.9 x7.95	50.8x50.8 x2.79	63.5x63.5 x6.35
8.1	75x130 x4.5 Rec	38.1x38.1 x4.78	38.1x38.1 x4.78	38.1x38.1 x4.78	38.1x38.1 x4.78	76.2x76.2 x3.81	38.1x38.1 x3.18	38.1x38.1 x3.18
8.2	"	" reinforced	" reinforced	"	"	"	"	"
9	75x130 x4.5 Rec	50.8x50.8 x6.35	50.8x50.8 x6.35	50.8x50.8 x4.78****	50.8x50.8 x6.35	76.2x76.2 x3.81	38.1x38.1 x3.18	38.1x38.1 x3.18
10	75x130 x4.5 Rec	63.5x63.5 x6.35	63.5x63.5 x6.35	63.5x63.5 x6.35	63.5x63.5 x6.35	76.2x76.2 x3.81	38.1x38.1 x3.18	38.1x38.1 x3.18

Notes: *2.79 wall thickness supplied instead of 3.81
**3.81 wall thickness supplied instead of 2.79
***3.81 wall thickness supplied instead of 3.18
****4.78 wall thickness supplied instead of 6.35

Table 1. Member Nominal Sizes

Specimen No.	α [deg]	θ [deg]	g [mm]	$\frac{g}{b_0}$	e [mm]	$\beta = \frac{b_1 + b_2}{2b_0}$	$\frac{b_0}{t_0}$
1	90°	45°	25	0.20	0	0.4	25.6
2	90°	45°	0	0.00	-52	0.4	25.4
3	90°	45°	51	0.40	+13	0.6	25.6
4	60°	39°	67	0.53	+13	0.6	25.2
5	90°	45°	25	0.20	0	0.4	15.8
6	60°	37°	73	0.57	- 4.8	0.4	26.6
7	90°	45°	56	0.44	+19.1	0.6	16.0
8	60°	38°	62	0.83*	-17.5	0.51*	16.6*
9	60°	38°	62	0.83*	- 7.9	0.68*	16.6*
10	60°	38°	62	0.83*	0	0.85*	16.6*

Notes: α = angle between web planes
θ = angle between diagonal web members and tension chord
g = gap dimension
e = eccentricity
*b_0 is based upon the width of one face of the hexagonal sections

Table 2. Joint Parameters. (Measured Values)

Material	Specification	Specified Properties: Minimum Yield Strength [MPa]	Specified Properties: Tensile Strength [MPa]	Specified Properties: Minimum Elongation [%]
Square HSS	Canadian: CSA G40.20, Class H; CSA G40.21, Grade 50W	345	488-621	22 in 50.8 mm
Hexagonal HSS	French: E-21 Steel	240	-	20 in 5.65 $\sqrt{S}$

Table 3. Specified Material Properties

Truss no.	Member Designation	Nominal Size (Supplied)	Yield Strength at 0.2% Offset [MPa]	Ultimate Strength [MPa]	Elongation [% in 50.8 mm]	Reduction of Area at Fracture [%]
1	B.C.	127.0x127.0x4.78	361	456	32	N.A.
	C.W.M. S1	50.8x50.8x2.79	330	484	25	N.A.
	C.W.M. S2	50.8x50.8x3.81	[illegible]	[illegible]	23	N.A.
	T.W.M. S1	50.8x50.8x2.79	334	481	25	N.A.
	T.W.M. S2	50.8x50.8x3.81	[illegible]	529	23	N.A.
2	B.C.	127.0x127.0x4.78	372	469	24	N.A.
	C.W.M. S1	50.8x50.8x2.79	330	464	25	N.A.
	C.W.M. S2	50.8x50.8x2.79	330	464	25	N.A.
	T.W.M. S1	50.8x50.8x2.79	330	[illegible]	25	N.A.
	T.W.M. S2	50.8x50.8x2.79	330	494	25	N.A.
3	B.C.	127.0x127.0x4.78	372	469	33	N.A.
	C.W.M.-S1	76.2x76.2x3.81	331	493	27	N.A.
	C.W.M. S2	76.2x76.2x3.18	332	488	23	N.A.
	T.W.M.-S1	76.2x76.2x3.81	331	495	27	N.A.
	T.W.M. S2	76.2x76.2x3.81	331	495	27	N.A.
4	B.C.	127.0x127.0x4.78	358	[illegible]	26	N.A.
	C.W.M. S1	76.2x76.2x3.18	332	466	23	N.A.
	C.W.M. S2	76.2x76.2x3.18	332	466	23	N.A.
	T.W.M.-S1	76.2x76.2x3.81	331	493	27	N.A.
	T.W.M.-S2	76.2x76.2x3.81	331	493	27	N.A.
5	B.C.	127.0x127.0x7.95	407	N.A.	N.A.	N.A.
	C.W.M. S1	50.8x50.8x6.35	341	466	23	N.A.
	C.W.M.-S2	50.8x50.8x6.35	341	466	29	N.A.
	T.W.M. S1	50.8x50.8x3.81	331	493	27	N.A.
	T.W.M. S2	50.8x50.8x3.81	331	493	27	N.A.
6	B.C.	127.0x127.0x4.78	372	479	31	55
	C.W.M. S1	50.8x50.8x6.35	328	483	30	56
	C.W.M.-S2	50.8x50.8x6.35	333	501	27	56
	T.W.M.-S1	50.8x50.8x6.35	343	511	27	55
	T.W.M. S2	50.8x50.8x4.78	327	530	25	53

Truss no.	Member Designation	Nominal Size (Supplied)	Yield Strength at 0.2% Offset [MPa]	Ultimate Strength [MPa]	Elongation [% in 50.8 mm]	Reduction of Area at Fracture [%]
7	B.C.	127.0x127.0x7.95	391	495	[illegible]	62
	C.W.M.-S1	76.2x76.2x7.95	391	545	17	55
	C.W.M. S2	76.2x76.2x7.95	391	545	17	55
	T.W.M.-S1	76.2x76.2x7.95	491	548	17	55
	T.W.M. S2	76.2x76.2x7.95	491	548	17	55
8	B.C.	75x150x4.5 Hex	272	374	[illegible]	56
	C.W.M. S1	38.1x38.1x4.78	310	503	26	49
	C.W.M.-S2	38.1x38.1x4.78	335	529	25	46
	T.W.M.-S1	38.1x38.1x4.78	340	500	26	49
	T.W.M.-S2	38.1x38.1x4.78	338	529	25	46
9	B.C.	75x150x4.5 Hex	257	506	37	58
	C.W.M.-S1	50.8x50.8x6.35	326	483	30	56
	C.W.M. S2	50.8x50.8x6.35	326	480	30	56
	T.W.M. S1	50.8x50.8x4.78	357	430	25	52
	T.W.M. S2	50.8x50.8x4.78	326	460	30	52
10	B.C.	75x150x4.5 Hex	259	508	37	62
	C.W.M. S1	63.5x63.5x6.35	353	526	24	55
	C.W.M. S2	63.5x63.5x6.35	353	526	24	55
	T.W.M. S1	63.5x63.5x6.35	353	526	24	55
	T.W.M. S2	63.5x63.5x6.35	353	526	24	55

Table 4. Coupon Results for All Members for All Trusses

Test no.	Deflection at V = 100 kN [mm]				Ratio [%]		
	Experimental Values	Analysis (a)	Analysis (b)	Analysis (c)	Exp. (a)	Exp. (b)	Exp. (c)
6	6.0	5.612	5.577	5.862	107	108	102
7	4.1	4.139	4.123	4.172	99	99	98
8.1	8.8	8.590	8.551	9.251	105	105	97
8.2	7.4	7.315	7.259	7.934	101	102	93
9	6.1	5.543	5.314	5.888	110	115	104
10	4.0	4.591	4.565	5.028	87	88	80

Table 5. Experimental and Analytical Overall Deflection in Tests no. 6 to 10

Test no. 1 The joint on side 1 deformed by about 10 mm (not corrected). The compression web member on side 1 buckled.
Test no. 2-S The joint deformed by less than 2 mm on both sides (not corrected). The reinforced compression web member on side 2 underwent local and overall buckling. Unconnected walls remain plane.
Test no. 3 The joint on side 2 deformed by about 9 mm (not corrected). Unconnected walls deflected out of plane at joint. The compression web member on side 2 underwent local and overall buckling.
Test no. 4 The joint deformed by about 11 mm on both sides (not corrected). Unconnected walls severely deflected out of plane at joint. The compression web members almost buckled.
Test no. 5 The joint deformed by less than 1.5 mm on both sides (not corrected). The compression web member on side 1 buckled. The tension web members yielded.
Test no. 6 The joint on side 1 deformed by about 4.5 mm, corrected (11 mm, not corrected). Both compression web members buckled.
Test no. 7 The joint deformed by less than 1 mm on both sides (corrected). The bottom chord reached first yield in shear but did not show significant shear distress. Test rig capacity reached prior to significant distress of test specimen.
Test no. 8-2 The joint deformed by about 22 mm on both sides (corrected). The bottom chord yielded in shear and in tension. Chord cross-section collapse under compression web member
Test no. 9 The joints deformed by about 20 mm (corrected). The bottom chord yielded; extreme shear deformation in gap. Cross-section collapse under compression web member. The chord walls fractured at walls at toe of tension web members
Test no. 10 The joint deformed only a little on both sides. The bottom chord yielded; extreme shear deformation in gap. The chord walls cracked at toe of tension web members.

Table 6. Summary of the Behaviour and Failure Modes in Tests 1 to 10

Test no. 1		
Maximum Applied Shear Load in Test [kN]		125.9
Joint Resistance [kN]	1%	93.2
	Yield	92.1
	Sheffield	128.7
	Corby	184.6
	Delft	163.8
	Packer	170.8
	B.C. Shear First Yield	231.
	Full Yield	349.
Member Resistance [kN]	T.B.C.	301.3
	C.W.M. Loc. Buck. M1	138.7
	M2	185.0
	C.W.M. S1 cl K = 0.7	152.6
	K = 0.9	129.0
	K = 0.77	145.2
	C.W.M. S2 cl K = 0.7	204.4
	K = 0.9	166.4
	K = 0.77	192.4
	T.W.M. S1	178.2
	S2	243.6

Table 7. Test no. 1 Shear Loads on Truss for Various Joint and Member Resistances

Test no. 2-s		
Maximum Applied Shear Load in Test [kN]		155.6
Joint Resistance [kN]	1%	-
	Yield	-
	Sheffield	135.2
	Corby	191.3
	Delft	173.2
	Packer	-
	B.C. Shear First Yield	243.
	Full Yield	367.
Member Resistance [kN]	T.B.C.	316.5
	C.W.M. Loc. Buck. M1	141.8
	M2	154.6
	C.W.M. S1 cl K = 0.7	158.1
	(reinforced) K = 0.9	134.0
	K = 0.77	150.5
	C.W.M. S2 cl K = 0.7	151.6
	(reinforced) K = 0.9	128.3
	K = 0.77	144.3
	T.W.M. S1	178.2
	S2	172.6

Table 8. Test no. 2-s Shear Loads on Truss for Various Joint and Member Resistances

Test no. 3		
Maximum Applied Shear Load in Test [kN]		288.6
Joint Resistance [kN]	1%	168.5
	Yield	168.5
	Sheffield	208.1
	Corby	361.5
	Delft	250.3
	Packer	333.0
	B.C. Shear First Yield	234.
	Full Yield	353.
Member Resistance [kN]	T.B.C.	260.1
	C.W.M. Loc. Buck. M1	236.0
	M2	315.2
	C.W.M. S1 cl K = 0.7	357.6
	K = 0.9	338.1
	K = 0.94	333.5
	C.W.M. S2 cl K = 0.7	289.1
	K = 0.9	273.3
	K = 0.94	269.5
	T.W.M. S1	365.9
	S2	364.4

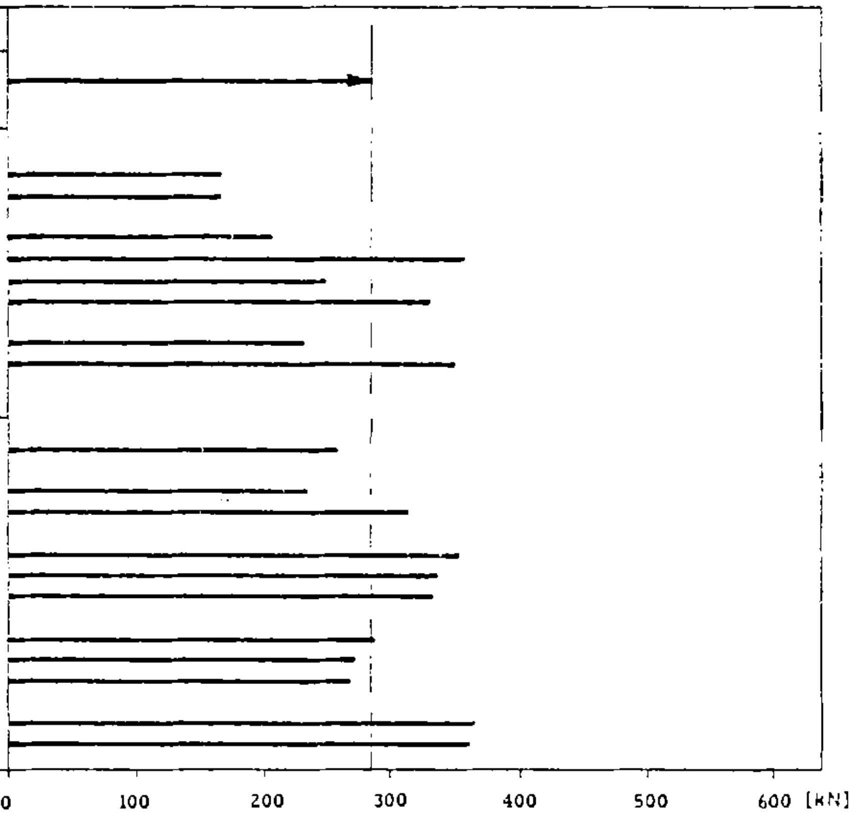

Table 9. Test no. 3 Shear Loads on Truss for Various Joint and Member Resistances

Test no. 4		
Maximum Applied Shear Load in Test [kN]		281.5
Joint Resistance [kN]	1%	240.2
	Yield	237.9
	Sheffield	253.9
	Corby	437.6
	Delft	292.3
	Packer	520.8
	B.C. Shear First Yield	235.
	Full Yield	355.
Member Resistance [kN]	T.B.C.	305.9
	C.W.M. Loc. Buck. M1	306.1
	M2	364.9
	C.W.M. S1 cl K = 0.7	339.4
	K = 0.9	324.7
	K = 0.96	319.2
	C.W.M. S2 cl K = 0.7	327.6
	K = 0.9	313.5
	K = 0.96	308.3
	T.W.M. S1	401.3
	S2	366.5

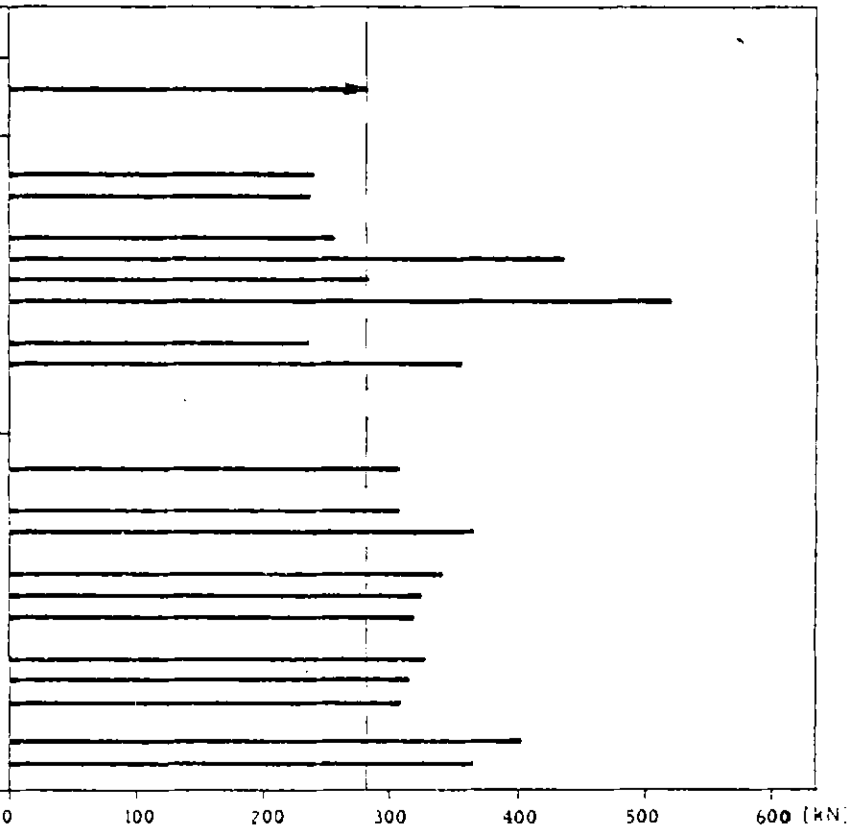

Table 10. Test no. 4 Shear Loads on Truss for Various Joint and Member Resistances

Test no. 5		
Maximum Applied Shear Load in Test [kN]		238.5
Joint Resistance [kN]	5%	309.1
	Yield	309.4
	Sheffield	235.0
	Corby	235.1
	Delft	361.3
	Parker	455.2
	B.C. Shear First Yield	408.
	Full Yield	616.
Member Resistance [kN]	T.B.C.	531.4
	C.W.M. Loc. Buck. M1	387.7
	M2	259.2
	C.W.M. S1 cl K = 0.7	281.5
	K = 0.9	222.2
	K = 0.77	262.7
	C.W.M. S2 cl K = 0.7	281.3
	K = 0.9	222.3
	K = 0.77	262.6
	T.W.M. S1	246.2
	S2	245.4

0 100 200 300 400 500 600 [kN]

Table 11. Test no. 5 Shear Loads on Truss for Various Joint and Member Resistances

Test no. 6		
Maximum Applied Shear Load in Test [kN]		249.4
Joint Resistance [kN]	5%	122.0
	Yield	120.6
	Sheffield	154.9
	Corby	225.4
	Delft	230.8
	Parker	275.0
	B.C. Shear First Yield	220.
	Full Yield	333.
Member Resistance [kN]	T.B.C.	287.1
	C.W.M. Loc. Buck. M1	328.3
	M2	320.4
	C.W.M. S1 cl K = 0.7	307.5
	K = 0.9	259.9
	K = 0.79	287.3
	C.W.M. S2 cl K = 0.7	311.1
	K = 0.9	258.8
	K = 0.79	289.6
	T.W.M. S1	373.4
	S2	320.7

0 100 200 300 400 500 600 [kN]

Table 12. Test no. 6 Shear Loads on Truss for Various Joint and Member Resistances

Test no. 7-2		
Maximum Applied Shear Load in Test [kN]		441.5
Joint Resistance [kN]	1%	816.7
	Yield	810.5
	Sheffield	360.5
	Corby	500.8
	Delft	651.5
	Packer	977.4
	B.C. Shear First Yield	382.
	Full Yield	577.
Member Resistance [kN]	T.B.C.	497.2
	C.W.M. Loc. Buck. M1	1067.1
	M2	1073.8
	C.W.M. S1 cl K = 0.7	811.1
	K = 0.9	723.9
	K = 0.94	703.2
	C.W.M. S2 cl K = 0.7	816.8
	K = 0.9	734.0
	K = 0.94	703.2
	T.W.M. S1	909.4
	S2	909.4

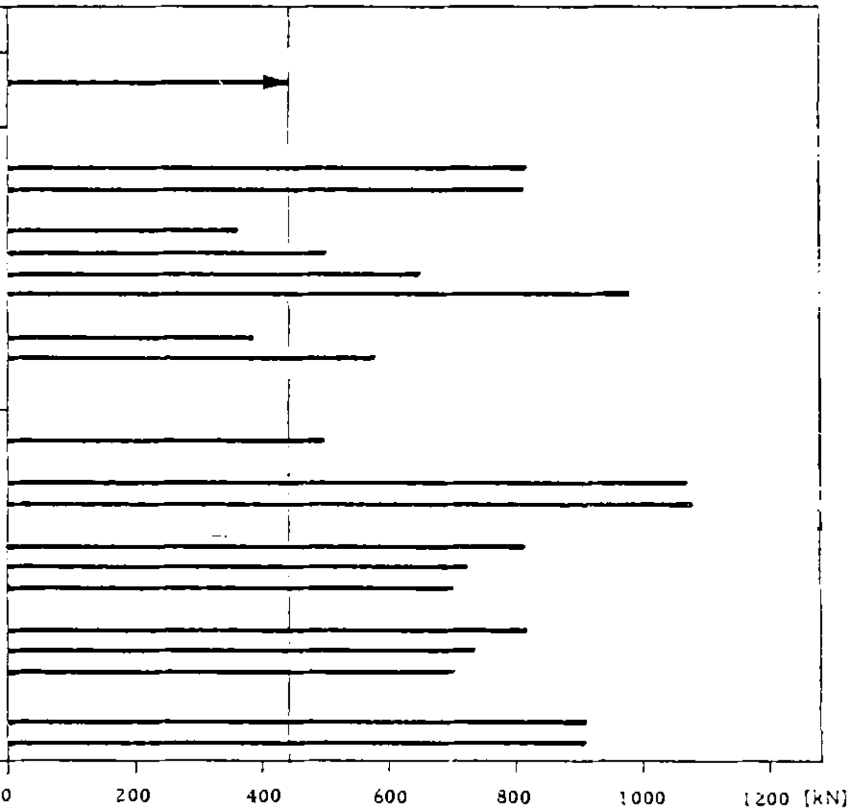

Table 13. Test no. 7-2 Shear Loads on Truss for Various Joint and Member Resistances

Test no. 8-2		
Maximum Applied Shear Load in Test [kN]		189.6
Joint Resistance [kN]	Steico d_0 = 130	> 211.0
	(CC) = 140	> 211.0
	Delft d_0 = 130	84.4
	(CC) = 140	83.4
	Sheffield b_0 = 75	115.5
	(RR) = 115	106.7
	Corby b_0 = 75	184.3
	(RR) = 115	-
	Delft b_0 = 75	147.3
	(RR) = 115	124.3
	B.C. Shear First Yield	146.8
	Full Yield	200.7
Member Resistance [kN]	T.B.C.	183.5
	C.W.M. S1 cl K = 0.7	318.5
	K = 0.9	265.1
	K = 0.74	309.1
	C.W.M. S2 cl K = 0.7	318.5
	K = 0.9	265.1
	K = 0.74	309.1
	T.W.M. S1	219.0
	S2	225.7

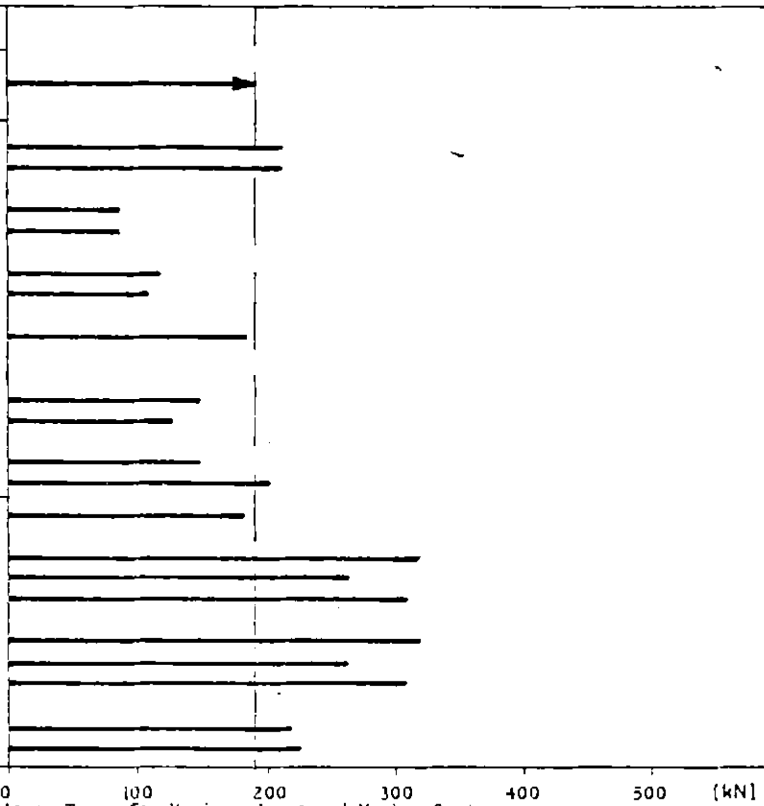

Table 14. Test no. 8-2 Shear Loads on Truss for Various Joint and Member Resistances

Test no. 9		
Maximum Applied Shear Load in Test [kN]		216.6
Joint Resistance [kN]	Stelco d_0 = 130 (CC)	> 310.5
	d_0 = 140	> 310.5
	Delft d_0 = 130 (CC)	96.3
	d_0 = 140	94.9
	Sheffield b_0 = 75 (RR)	215.4
	b_0 = 115	100.6
	Corby b_0 = 75 (RR)	301.0
	b_0 = 115	170.6
	Delft b_0 = 75 (RR)	181.3
	b_0 = 115	151.4
	B.C. Shear First Yield	138.0
	Full Yield	188.7
Member Resistance [kN]	T.B.C.	369.2
	C.B.C.	322.1
	C.W.M. S1 cl K = 0.7	308.5
	K = 0.9	260.9
	K = 0.86	271.6
	C.W.M. S2 cl K = 0.7	307.5
	K = 0.9	259.8
	K = 0.86	270.5
	T.W.M. S1	320.7
	S2	363.9

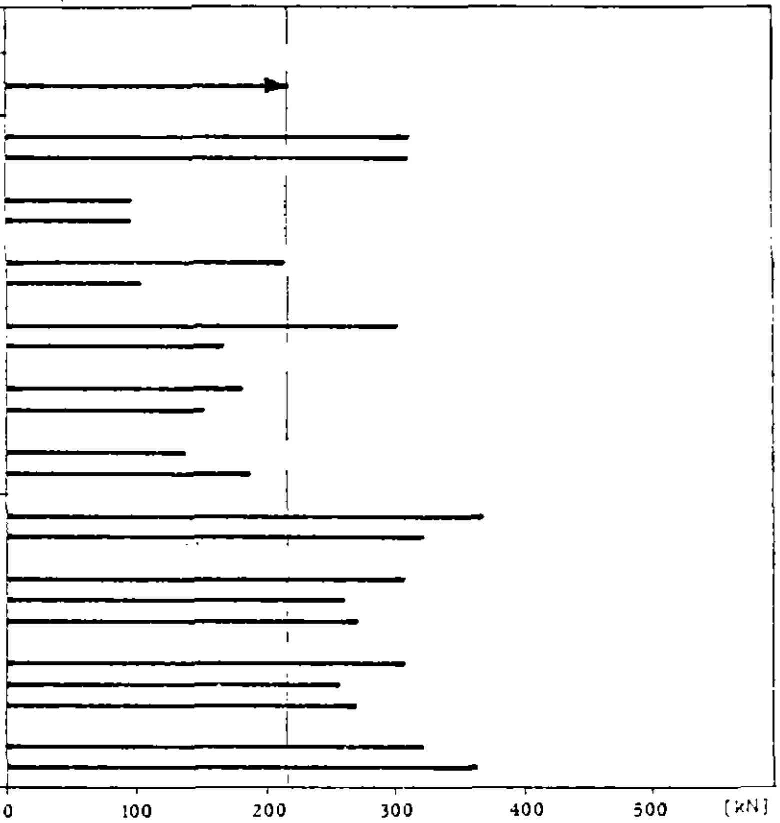

Table 15. Test no. 9 Shear Loads on Truss for Various Joint and Member Resistances

Test no. 10		
Maximum Applied Shear Load in Test [kN]		253.7
Joint Resistance [kN]	Stelco d_0 = 130 (CC)	485.2
	d_0 = 140	390.1
	Delft d_0 = 130 (CC)	117.2
	d_0 = 140	115.0
	Sheffield b_0 = 75 (RR)	325.8
	b_0 = 115	137.6
	Corby b_0 = 75 (RR)	433.3
	b_0 = 115	242.7
	Delft b_0 = 75 (RR)	228.7
	b_0 = 115	189.9
	B.C. Shear First Yield	140.9
	Full Yield	192.7
Member Resistance [kN]	T.B.C.	377.0
	C.B.C.	328.9
	C.W.M. S1 cl K = 0.7	459.4
	K = 0.9	418.9
	K = 0.96	404.2
	C.W.M. S2 cl K = 0.7	459.4
	K = 0.9	418.9
	K = 0.96	404.2
	T.W.M. S1	503.7
	S2	503.7

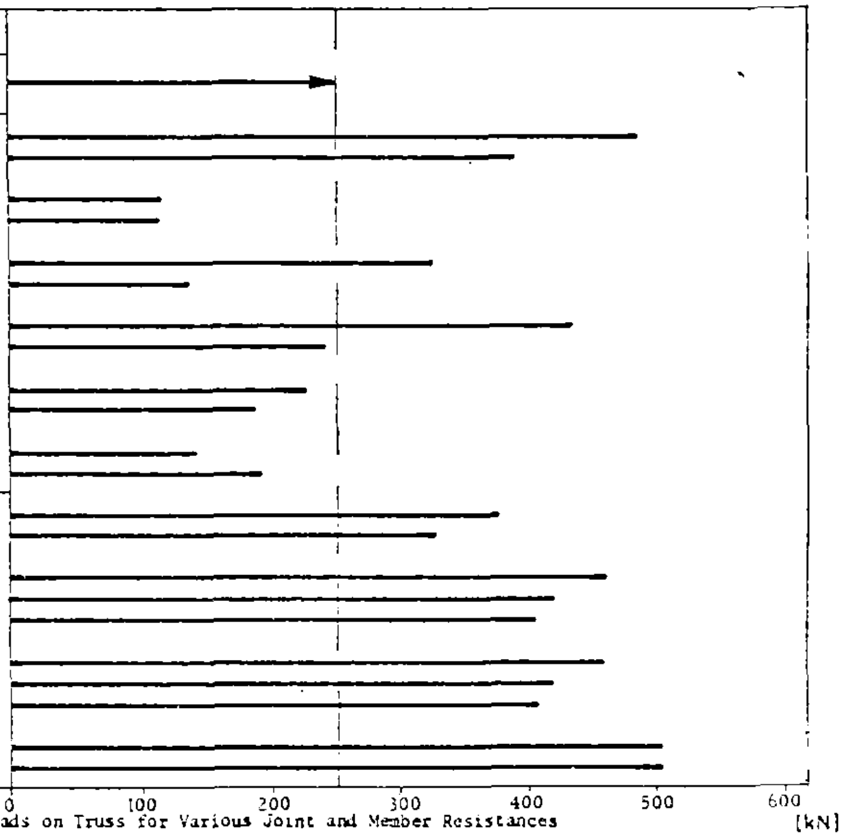

Table 16. Test no. 10 Shear Loads on Truss for Various Joint and Member Resistances

Failure Modes \ Test no.	1	2-s	3	4	5	6	7-2	8-1	8-2	9	10
Joint Deformations along the C.W.M.'s [mm]*	10	2	9	11	1.5	11 (4.5)	1 (1)	2 (1)	22 (22)	10 (10)	little (little)
Push-Pull Ultimate Failure	x								x	x	x
Shear Yielding of the Bottom Chord			x	x			impending		x	x	x
C.W.M. Buckling	x	x	x	impending	x	x		impending			
Predicted K (Ref. 13)	0.77	0.77	0.94	0.96	0.77	0.79	0.94	0.74	0.74	0.86	0.96
Backcalculated K	0.9		0.7		0.7	0.9		0.74			
Local Buckling		x	x								
Interaction Between Joint Deformations and C.W.M. Buckling	x		x	x		x		x			
B.C. Tension Yield							impending		x		
T.W.M. Yield					x						

Note: *bracketted terms are corrected values. The unbracketted terms may be compared directly with those given for Tests 1 to 5.

Table 17. Failure Modes in Tests no. 1 to 10

Specimen no.	Parameter Varied	g/b_0	β	b_0/t_0	α
1	$g = 0.44\ b_0$		0.4	26.6	90°
2	$= 0.0\ b_0$		0.4	26.6	90°
1	$\beta = 0.4$	0.44		26.6	90°
3	$= 0.6$	0.35		26.6	90°
5	$= 0.4$	0.44		16.0	90°
7	$= 0.6$	0.44		16.0	90°
6	$= 0.4$	0.60		26.6	60°
4	$= 0.6$	0.60		26.6	60°
1	$b_0/t_0 = 26.6$	0.44	0.4		90°
5	$= 16.0$	0.44	0.4		90°
3	$= 26.6$	0.35	0.6		90°
7	$= 16.0$	0.44	0.6		90°
1	$\alpha = 90°$	0.44	0.4	26.6	
6	$= 60°$	0.60	0.4	26.6	
3	$= 90°$	0.35	0.6	26.6	
4	$= 60°$	0.60	0.6	26.6	
8*	$\beta = 0.51$	0.83		16.6	60°
9*	$= 0.68$	0.83		16.6	60°
10*	$= 0.85$	0.83		16.6	60°

NOTES: * For specimens no. 8, 9 and 10, b_0 is assumed to be 75 mm.

Table 18. Comparisons Between the Joint Parameters (Nominal Values)

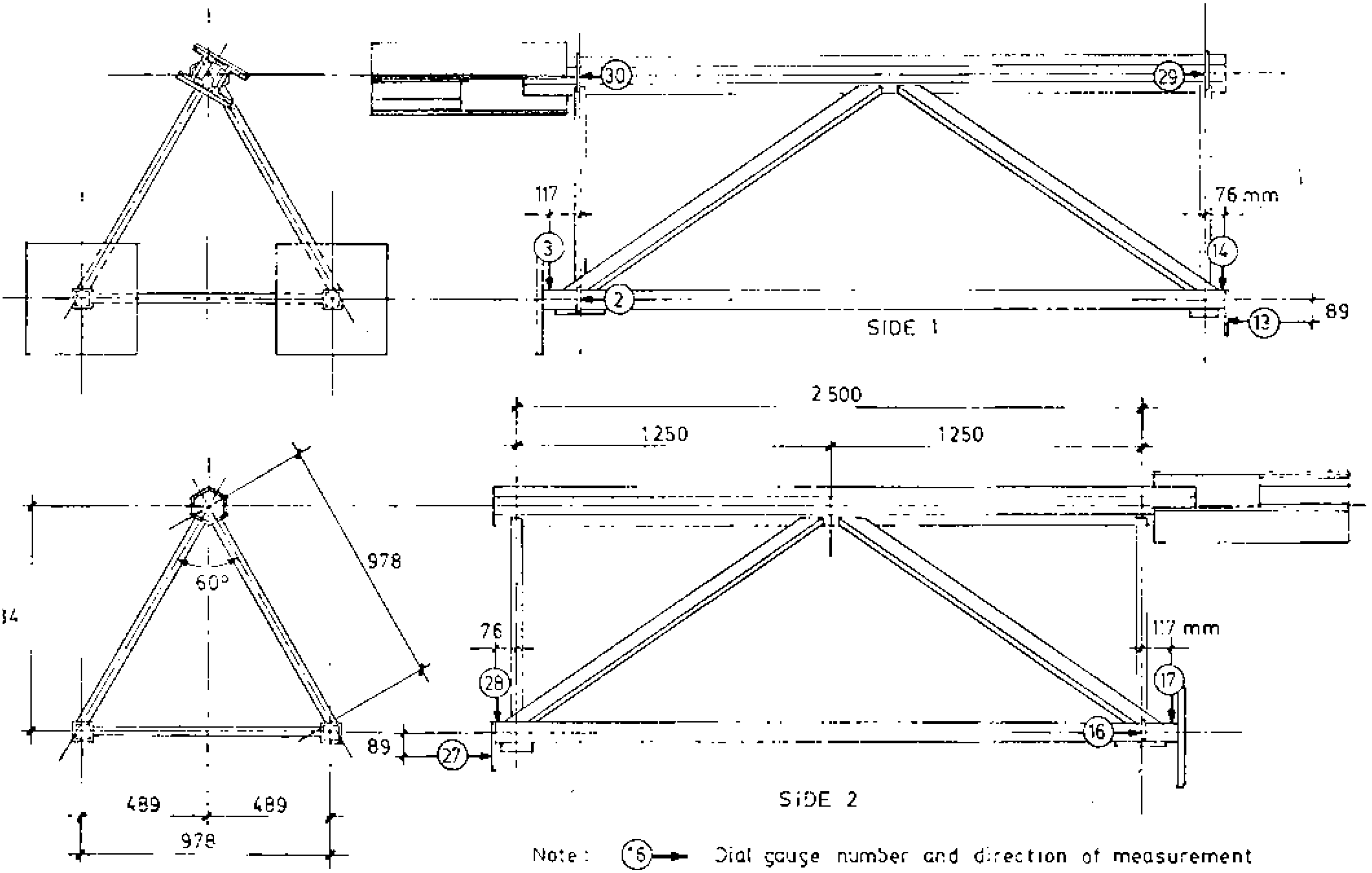

Figure 1. Nominal Truss Dimensions and Deflection Gauge Positions

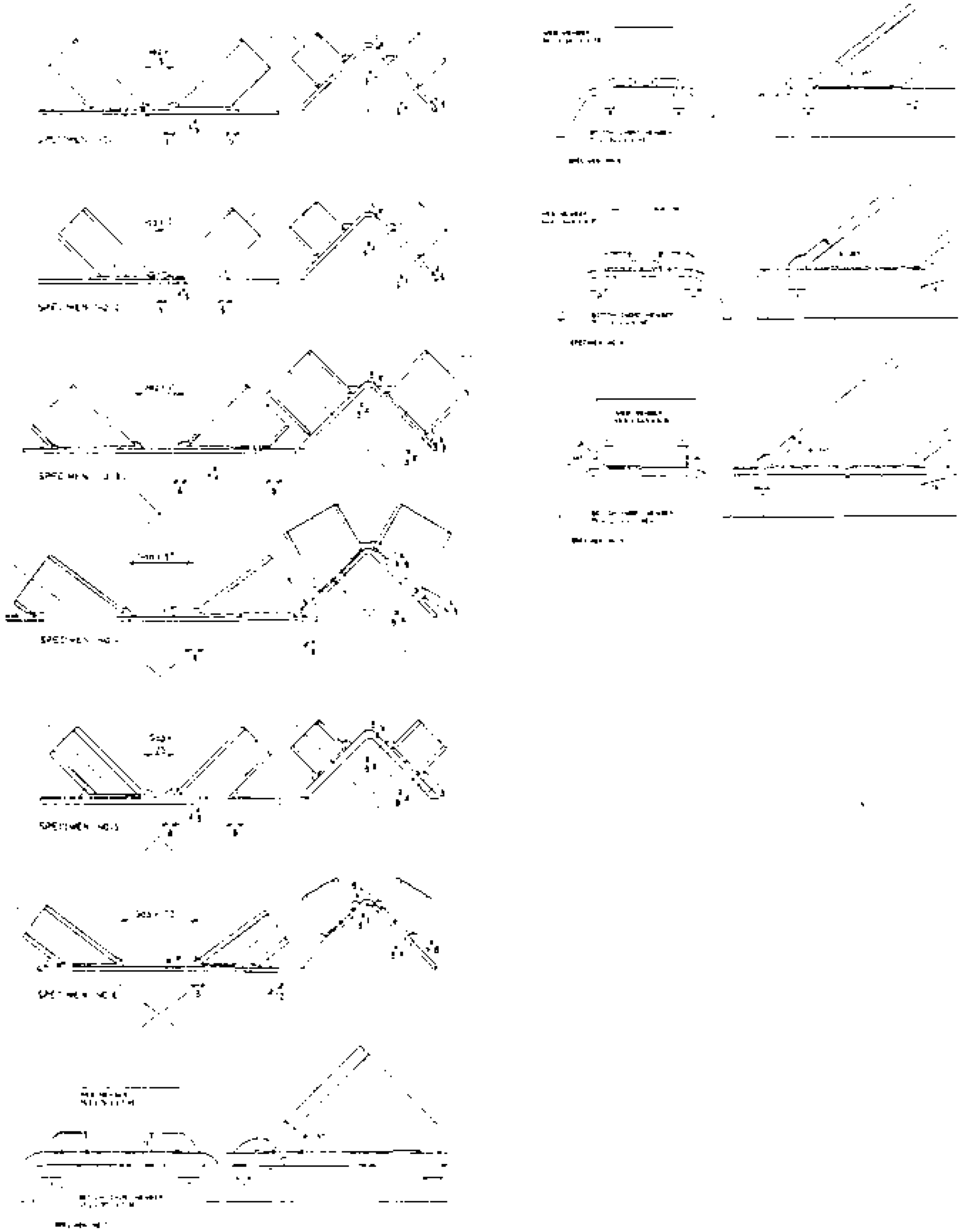

Fig. 2. Weld Details for Test Specimens

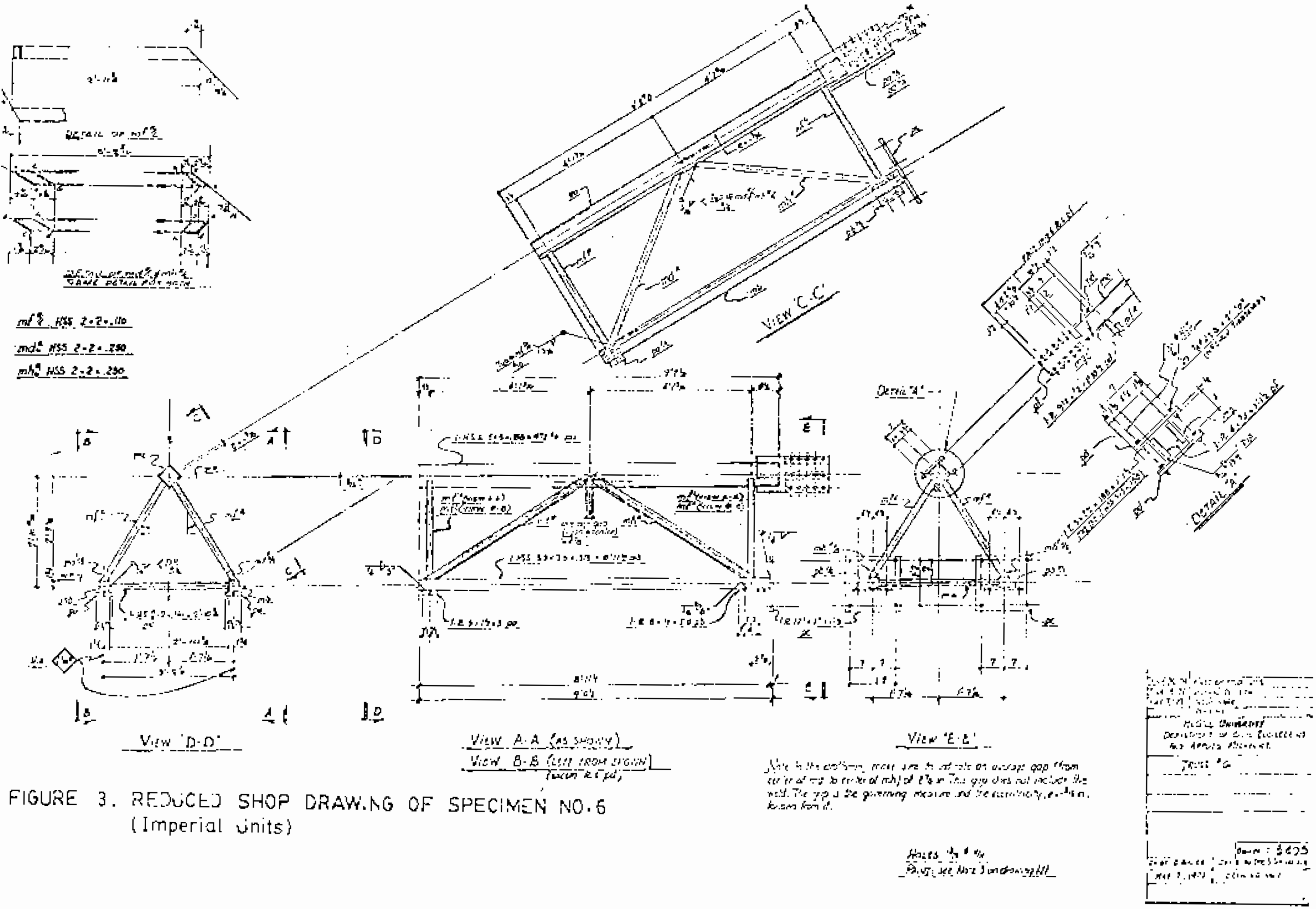

FIGURE 3. REDUCED SHOP DRAWING OF SPECIMEN NO. 6
(Imperial Units)

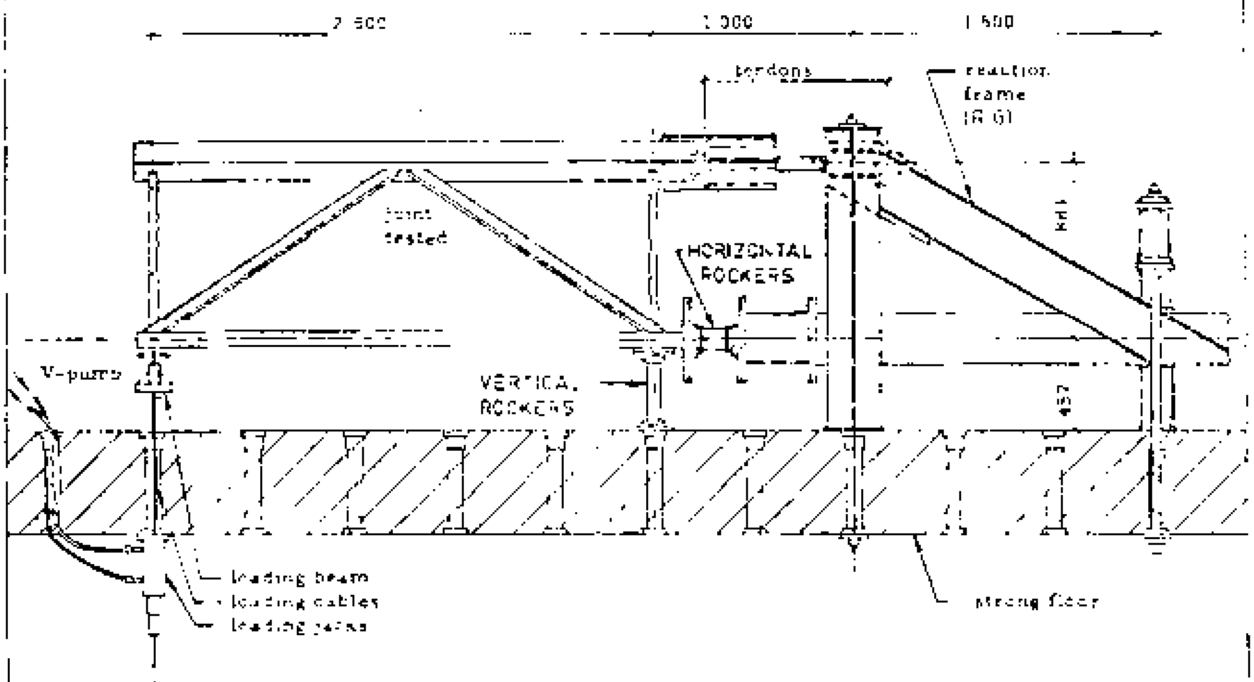

FIGURE 4. TESTING ARRANGEMENT WITHOUT PRESTRESSING OF THE BOTTOM CHORD
(TESTS NO. 1,2 4 - 8)

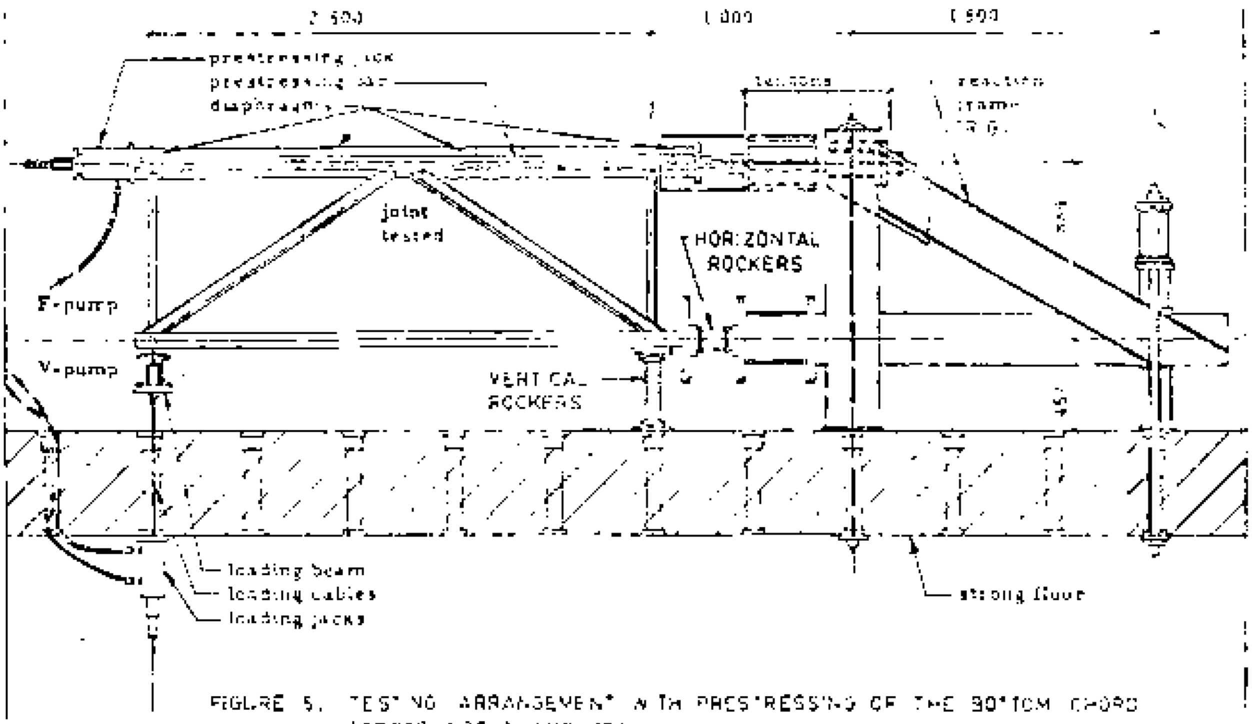

FIGURE 5. TESTING ARRANGEMENT WITH PRESTRESSING OF THE BOTTOM CHORD
(TESTS NOS. 9 AND 10)

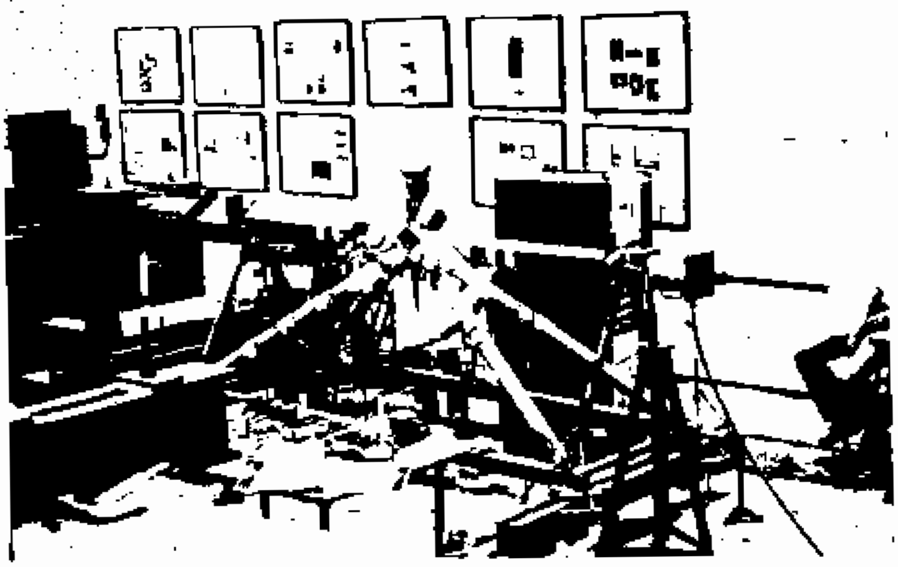

Figure 6. Fully Instrumented Specimen in Test Rig

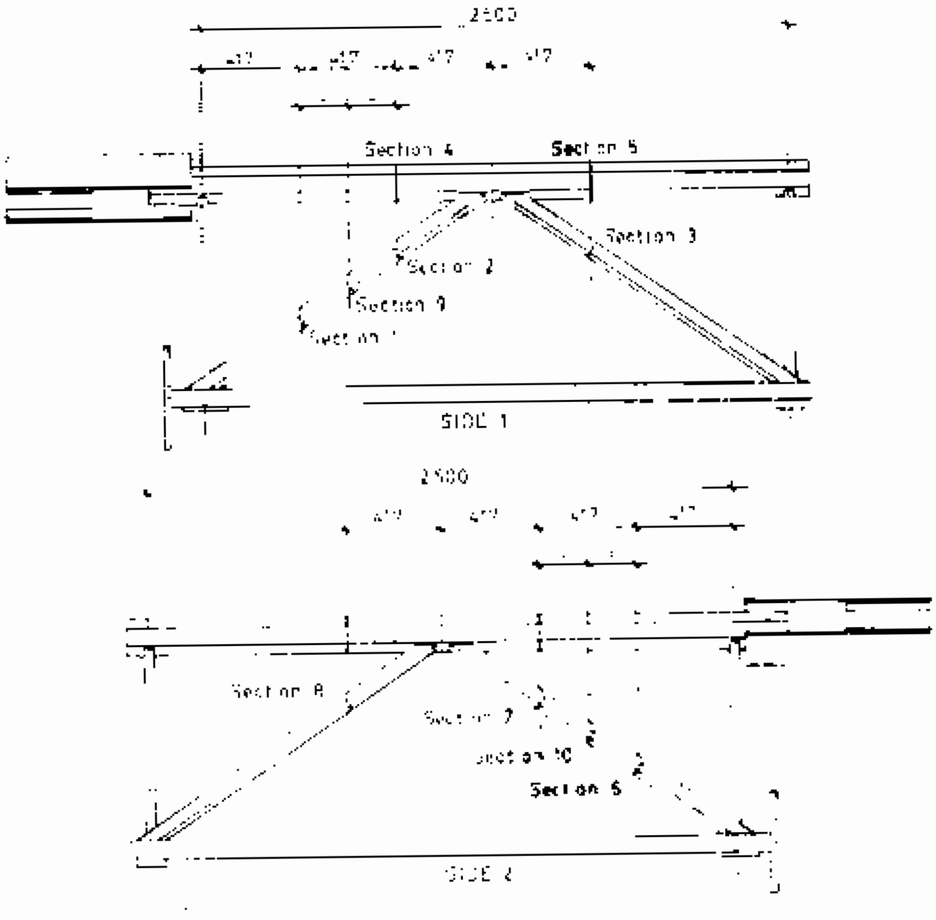

FIGURE 7. LOCATION OF THE ... STRAIN GAGE
ON SPECIMENS NOS 5 ...

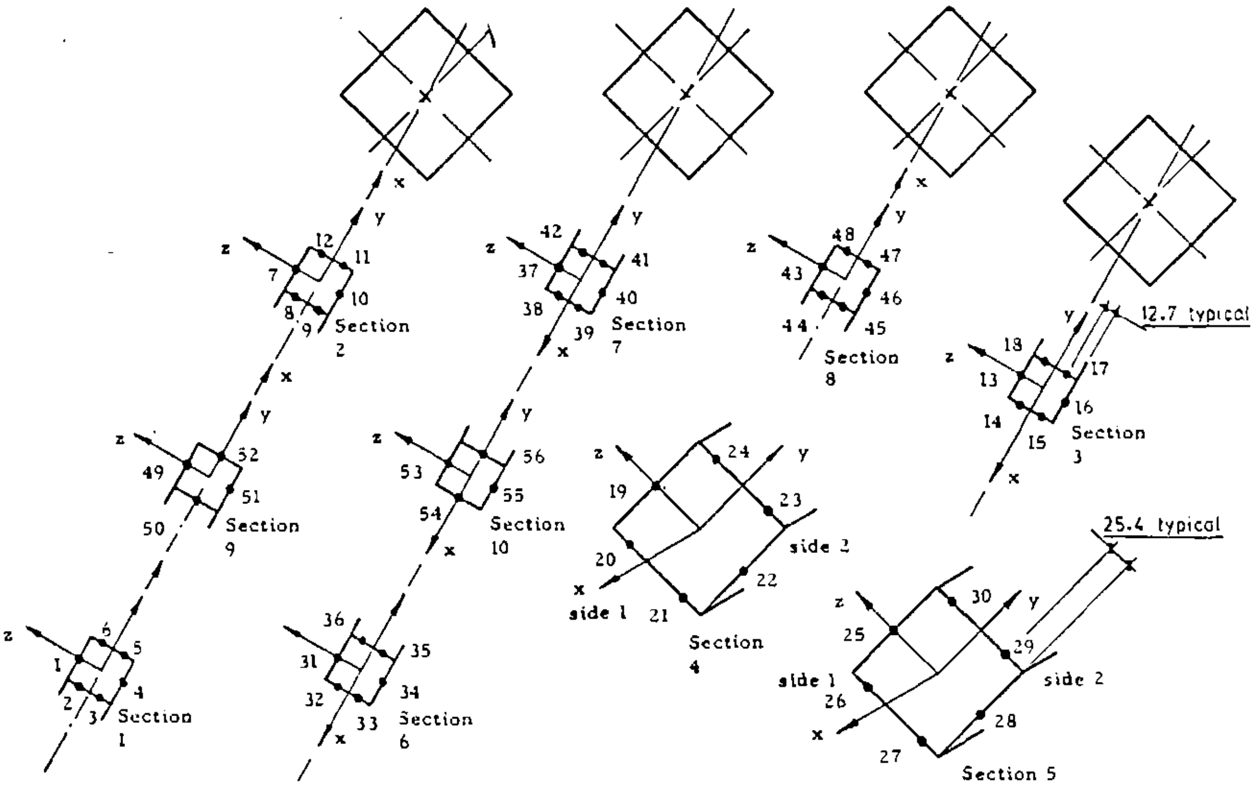

FIGURE 8 . STRAIN GAGE LOCATIONS ON SPECIMEN NO. 6

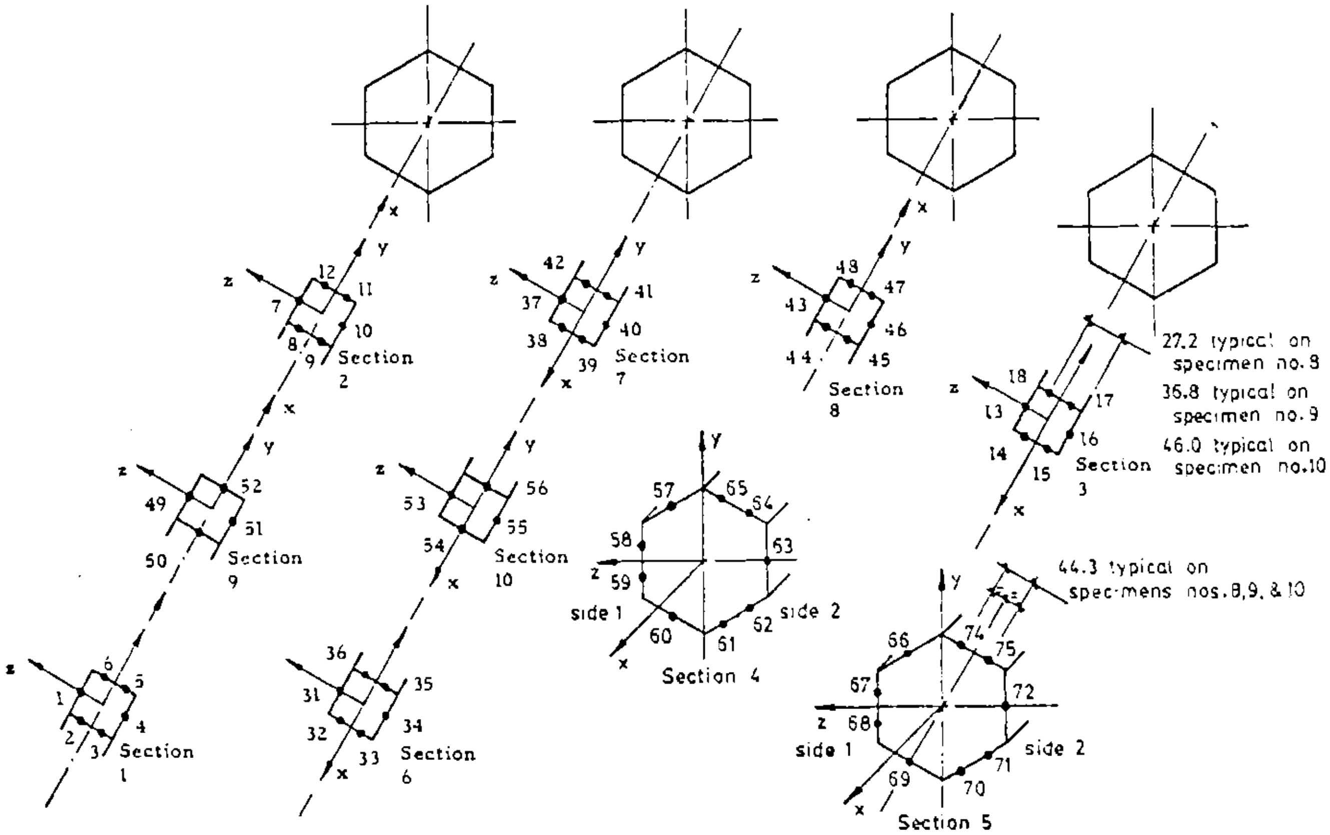

FIGURE 9 . STRAIN GAGE LOCATIONS ON SPECIMENS NOS. 8, 9, & 10

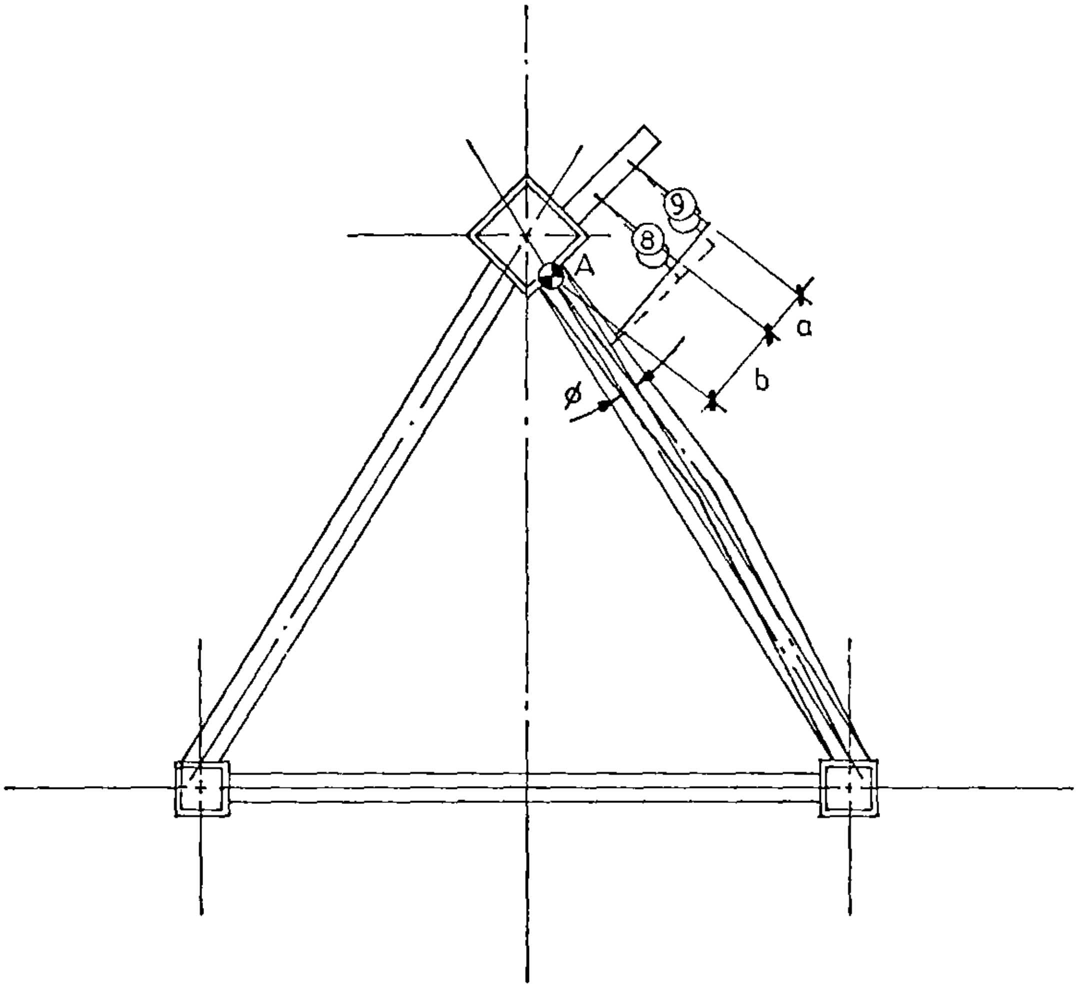

FIGURE 10 . OUT-OF-WEB-PLANE BENDING OF THE COMPRESSION WEB MEMBERS.

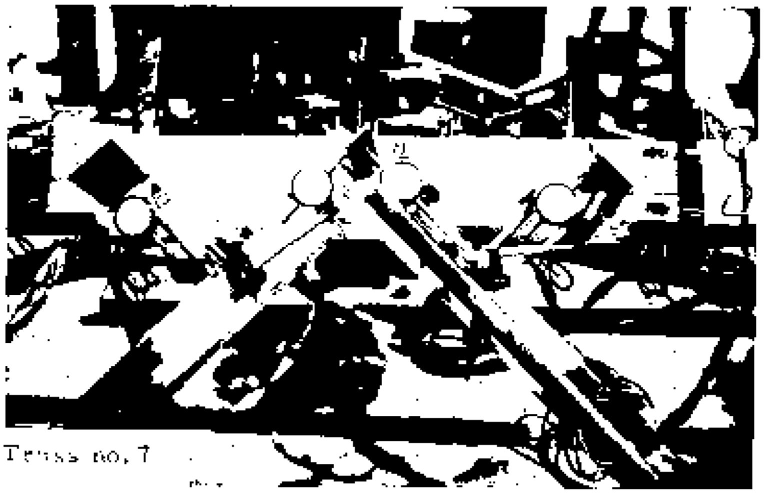

(a) Measurements of the Joint Deformations
(Tests nos. 6, 7 and 10)

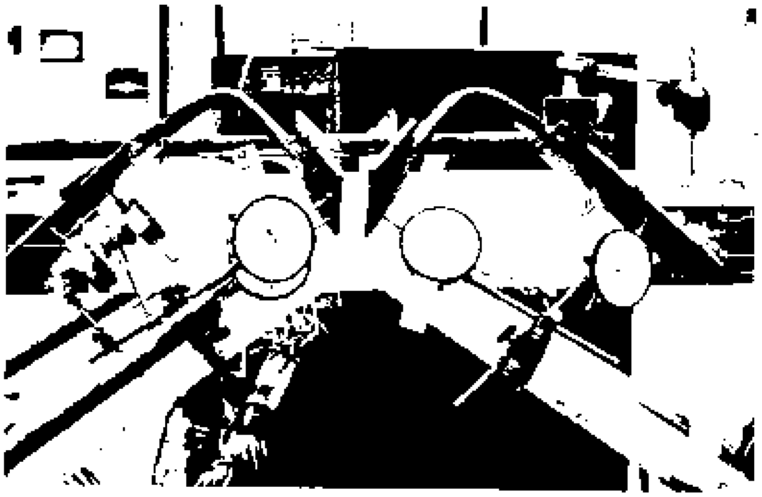

(b) Measurements of the Joint Deformations
(Tests nos. 8 and 9)

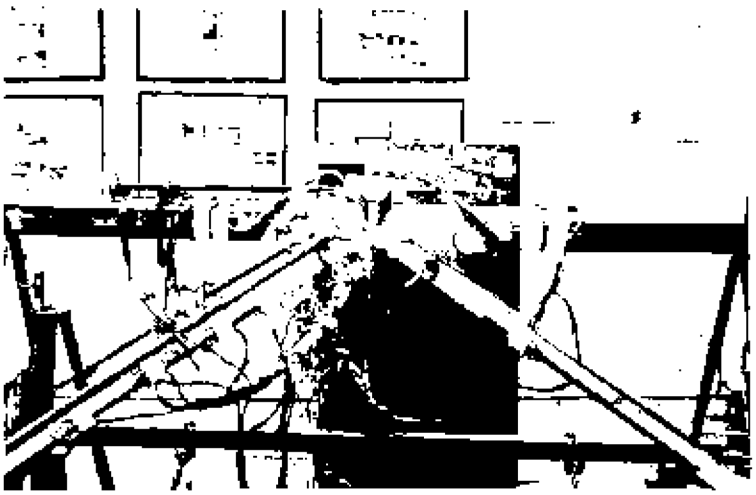

(c) Measurements of Bottom Chord Shear Deformations
(Tests nos. 8 and 9 only)

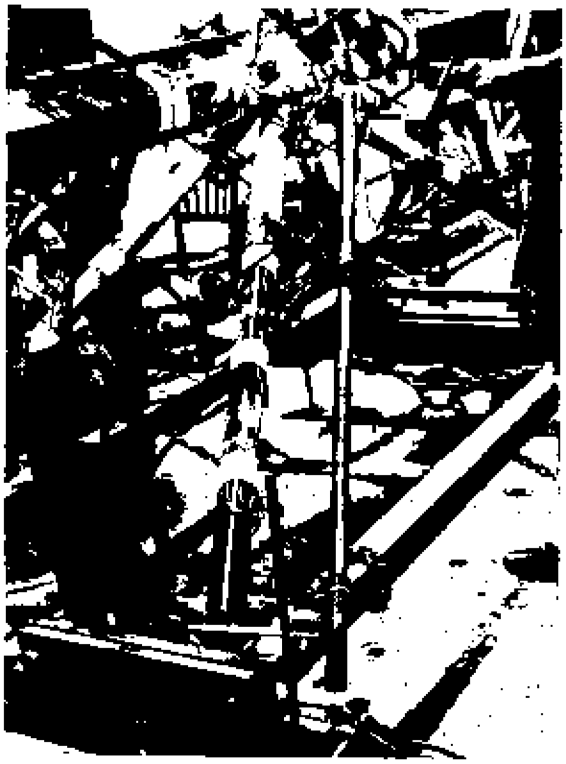

(d) Measurements of Mid-length
Transverse Deflections of the
Compression Web Members

Figure 11.

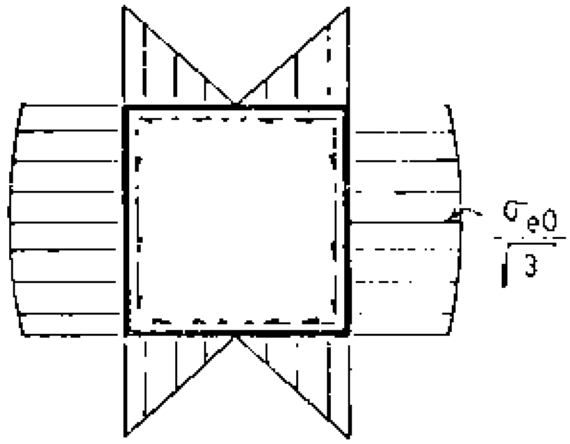

(a) PLANAR TRUSS. RHS CHORD. ELASTIC DISTRIBUTION

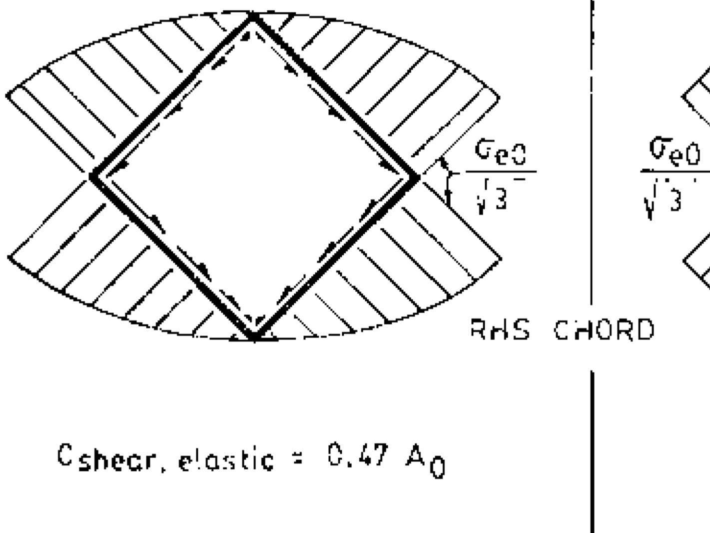

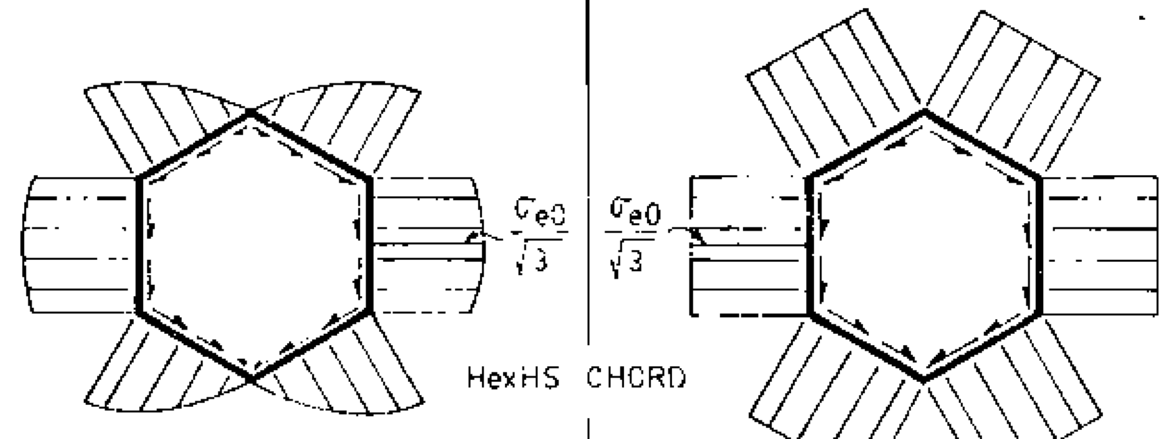

RHS CHORD

$C_{shear,\, elastic} = 0.47\ A_0$ | $C_{shear,\, plastic} = 0.71\ A_0$

HexHS CHORD

$C_{shear,\, elastic} = 0.48\ A_0$ | $C_{shear,\, plastic} = 0.67\ A_0$

(b) TRIANGULAR TRUSS. ELASTIC DISTRIBUTION

(c) TRIANGULAR TRUSS. PLASTIC DISTRIBUTION

FIGURE 12. ELASTIC AND PLASTIC SHEAR STRESS DISTRIBUTIONS IN RHS AND HexHS CHORDS. PLANAR AND TRIANGULAR TRUSSES

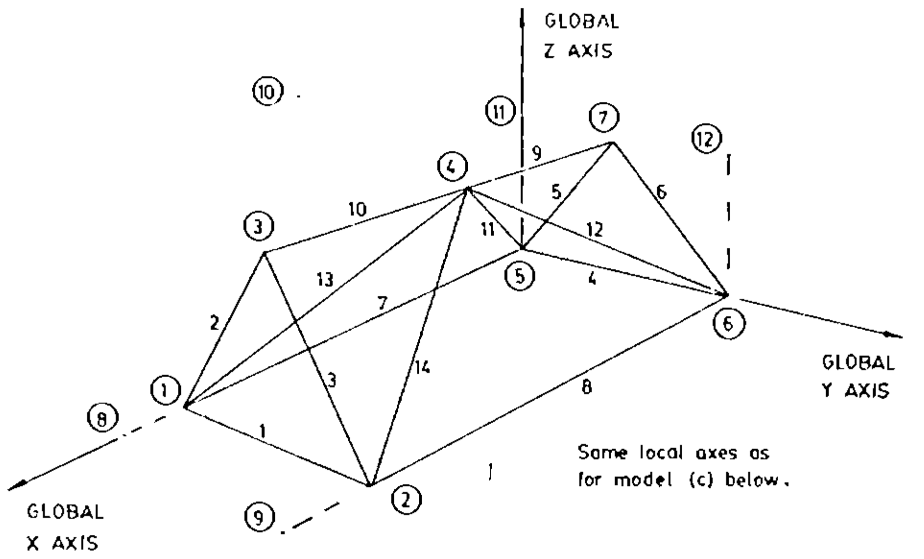

MODEL (a): PINNED JOINTS
MODEL (b): FIXED JOINTS WITH ZERO ECCENTRICITIES

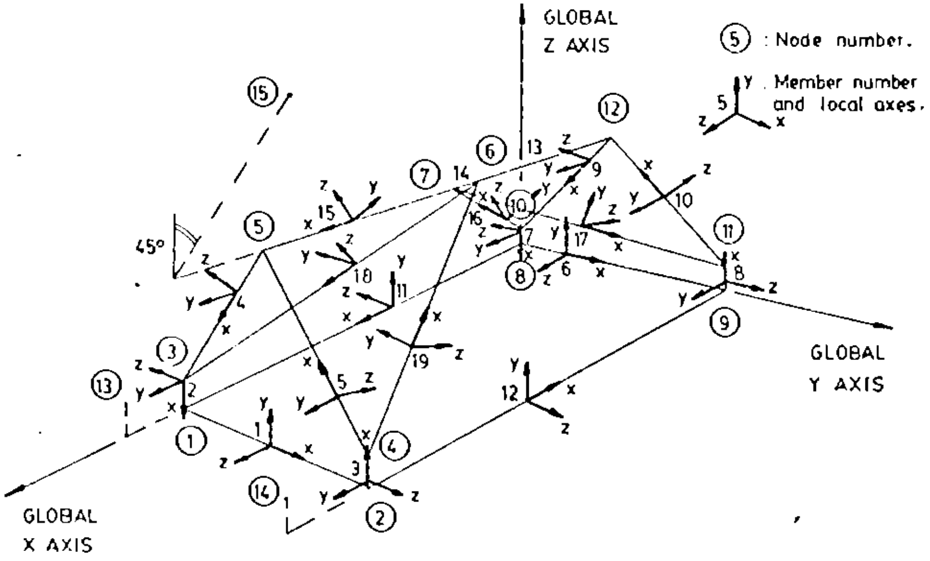

MODEL (c): FIXED JOINTS WITH APPROXIMATED ECCENTRICITIES

FIGURE 13. MODELS USED FOR THE SAP ANALYSES OF SPECIMEN NO. 6.

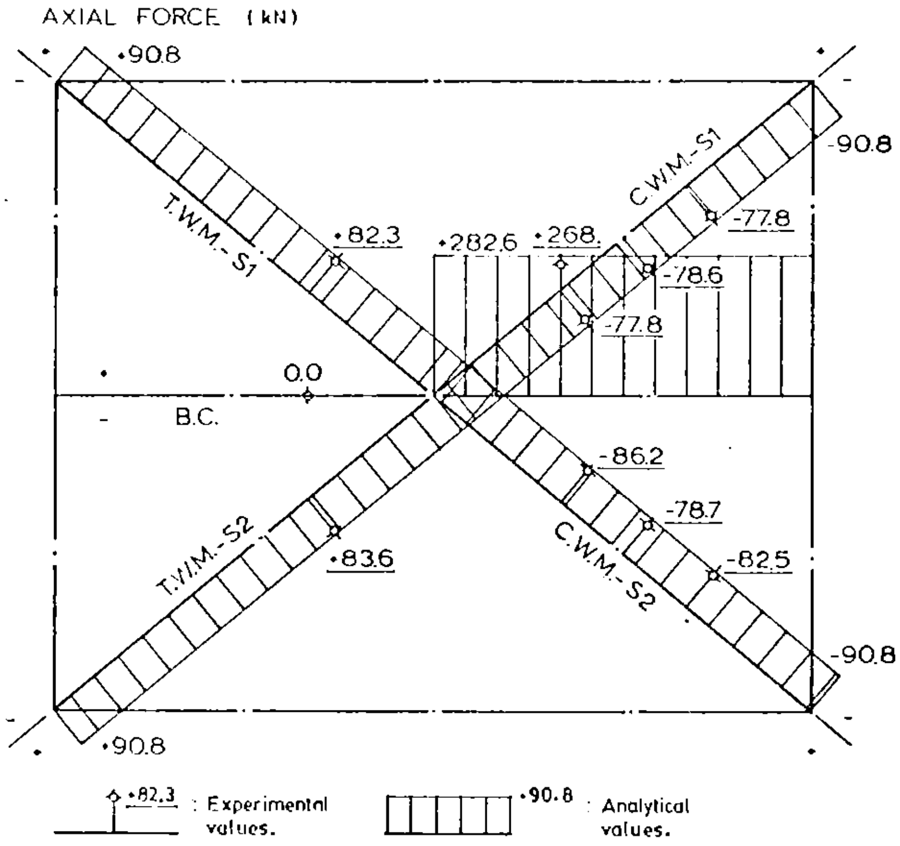

B.C.: Bottom chord
C.W.M.-S1, C.W.M.-S2 : Compression web member on side 1, on side 2.
T.W.M.-S1, T.W.M.-S2 : Tension " "

FIGURE 14. AXIAL FORCE DIAGRAM FOR TEST NO.6 AT V = 100 kN, EXPERIMENTAL VALUES AND ANALYTICAL VALUES FROM MODEL (a) (PINNED JOINTS)

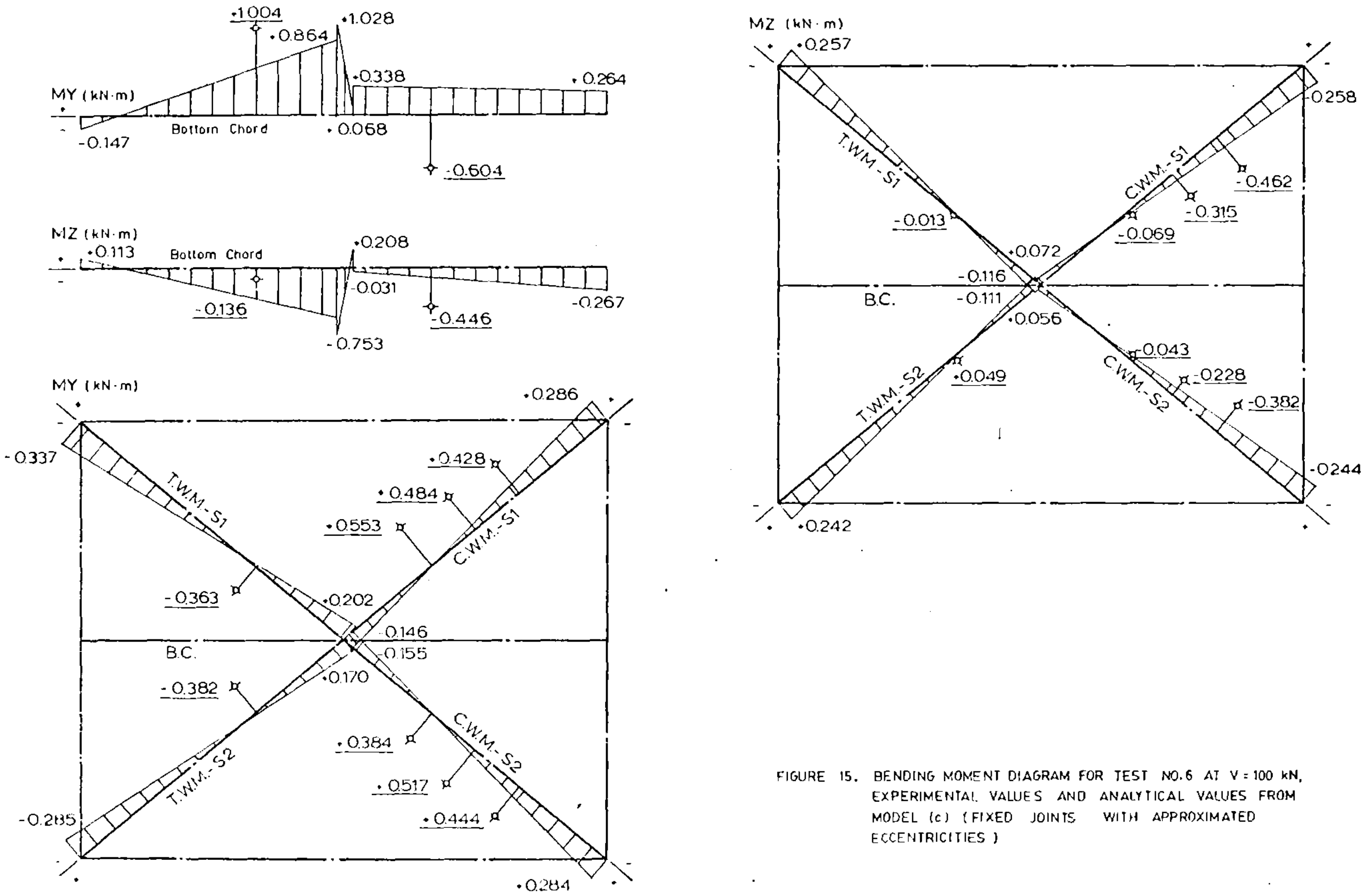

FIGURE 15. BENDING MOMENT DIAGRAM FOR TEST NO.6 AT V = 100 kN, EXPERIMENTAL VALUES AND ANALYTICAL VALUES FROM MODEL (c) (FIXED JOINTS WITH APPROXIMATED ECCENTRICITIES)

(a) Truss No. 1

(b) Truss No. 2

(c) Truss No. 3

(d) Truss No. 4

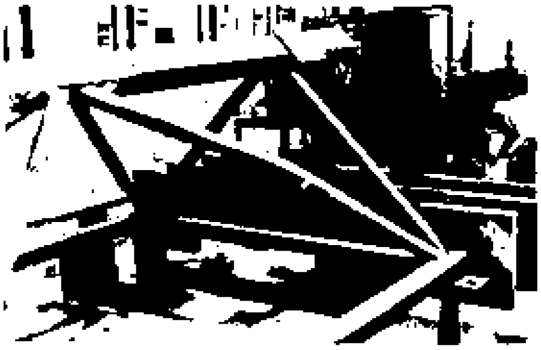

(e) Truss No. 5

(f) Truss No. 6

(g) Truss No. 8

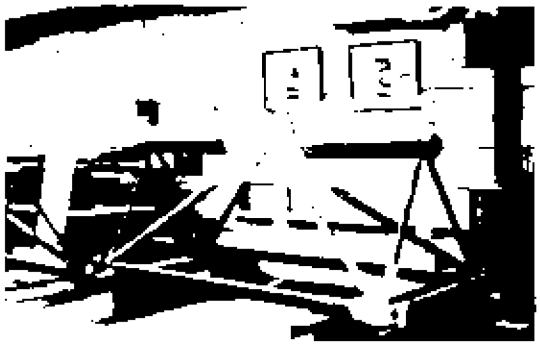

(h) Truss No. 9

(i) Truss No. 1

Figure 16. Trusses and Joints after Testing

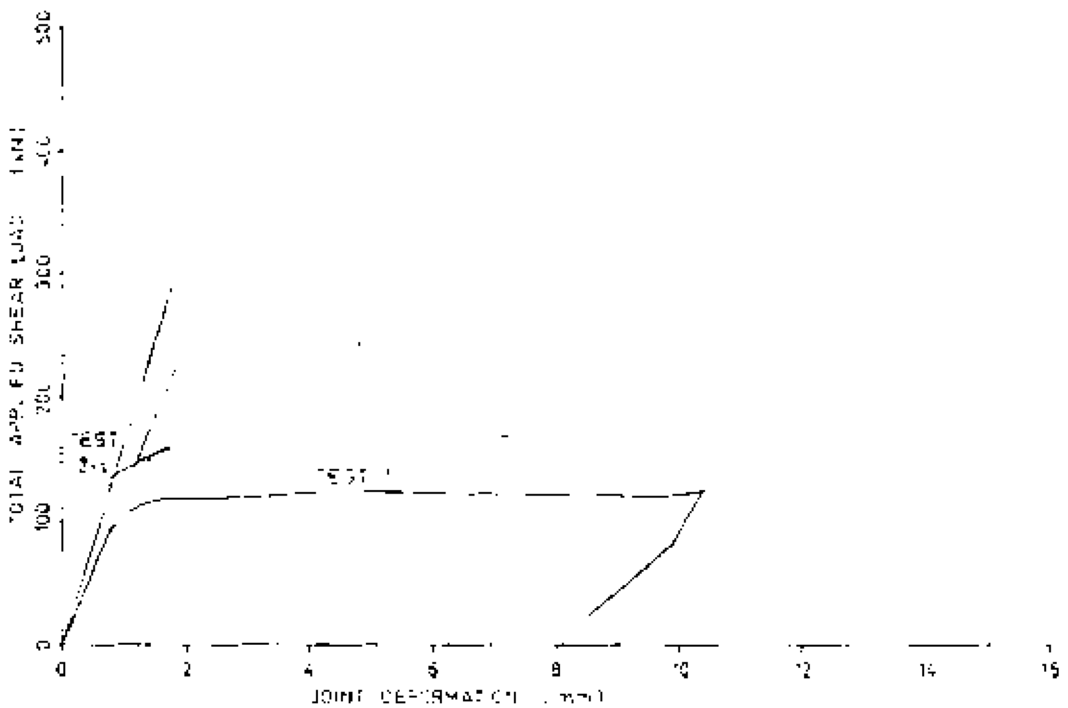

FIGURE 17a : TEST NO.1 – COMPRESSION - SIDE 1
TEST NO.2 – COMPRESSION - SIDE 2

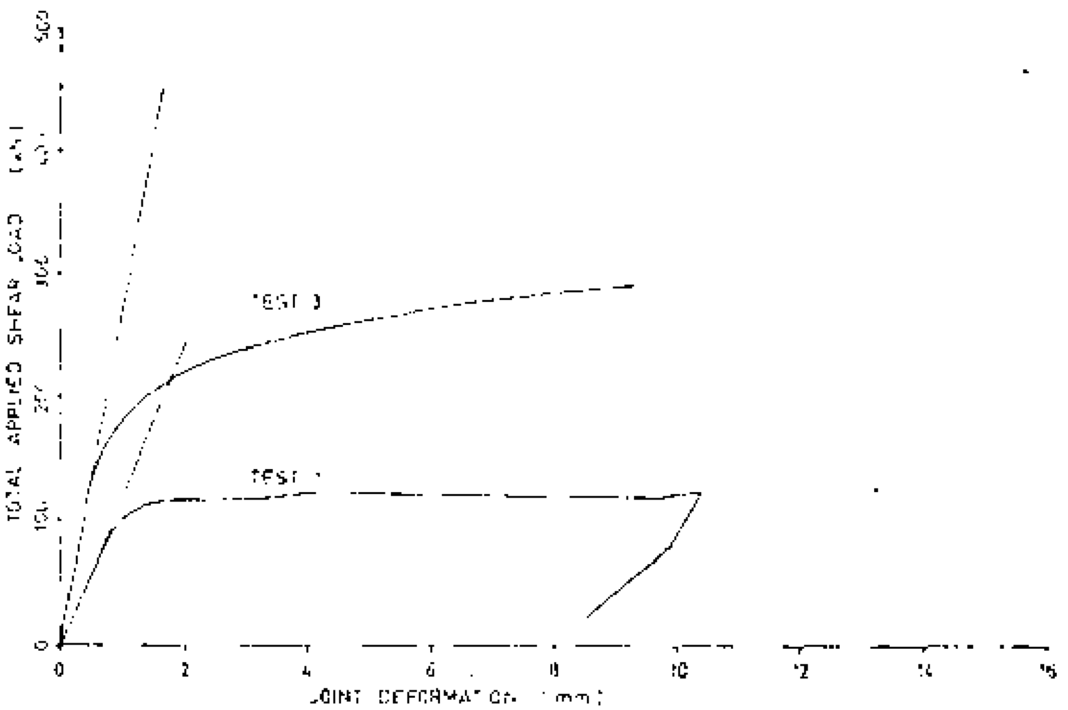

FIGURE 17b : TEST NO.1 – COMPRESSION - SIDE 1
TEST NO.3 – COMPRESSION - SIDE 2

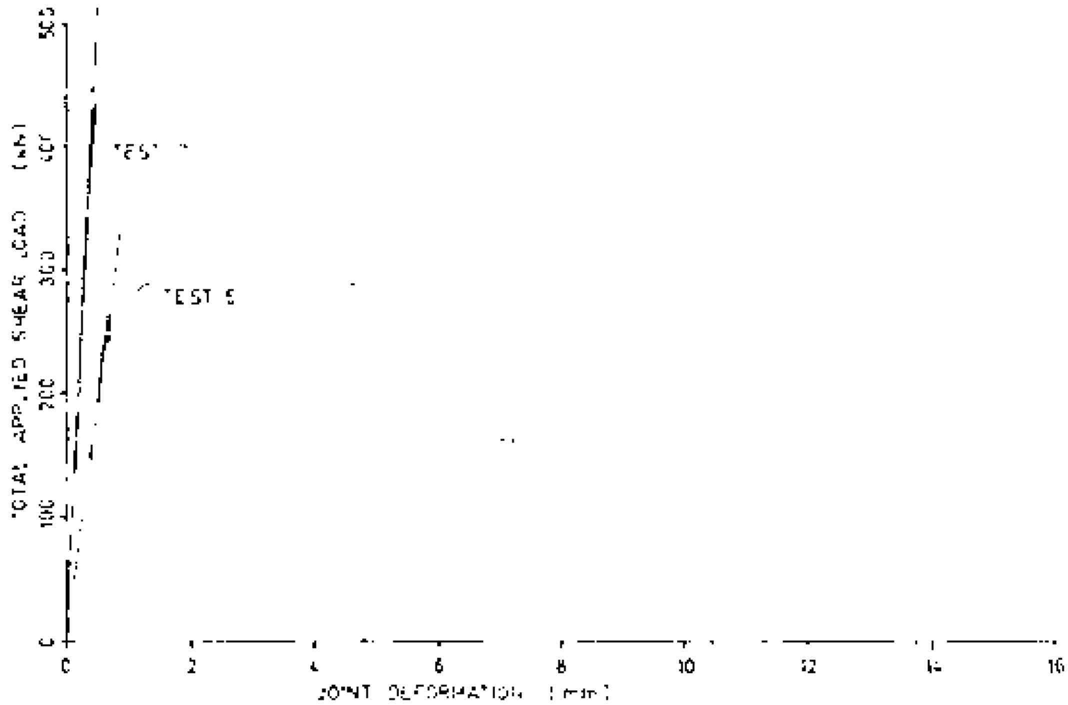

FIGURE 17c . TEST NO. 5 COMPRESSION-SIDE 1
TEST NO. 7 COMPRESSION-SIDE 1

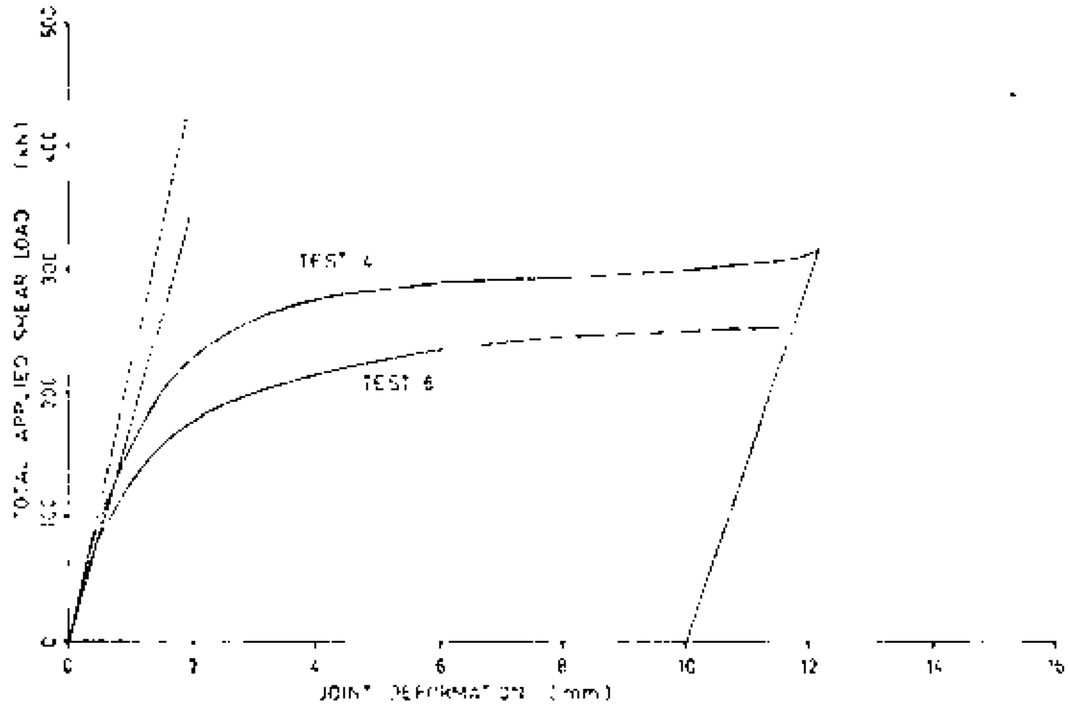

FIGURE 17d . TEST NO. 4 COMPRESSION-SIDE 2
TEST NO. 6 COMPRESSION-SIDE 1

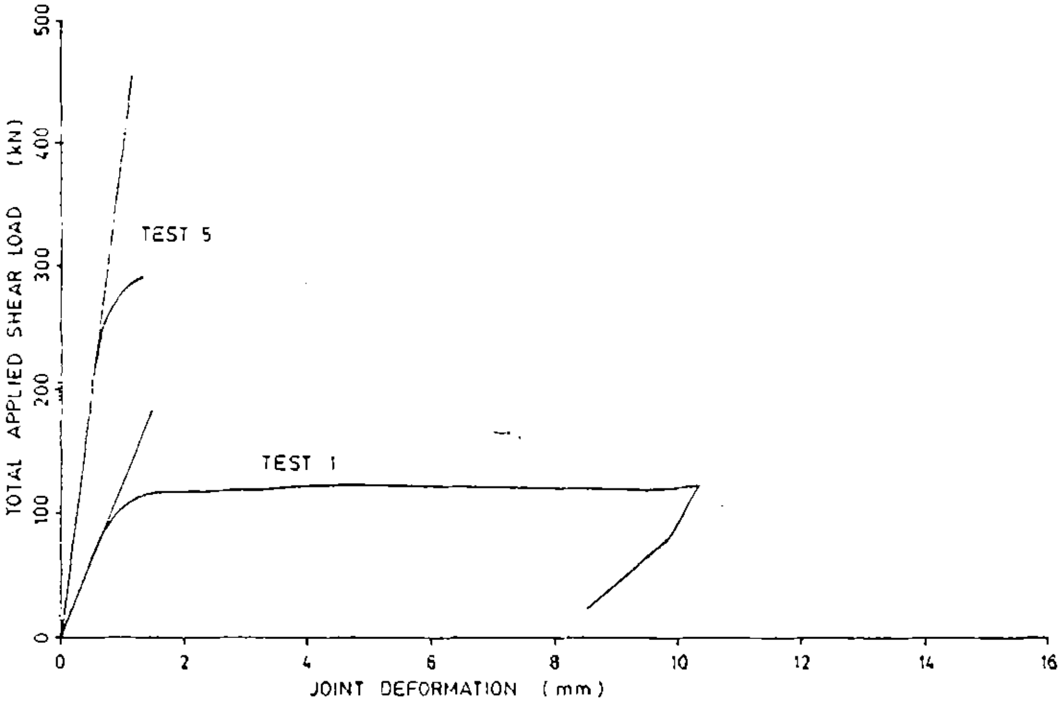

FIGURE 17e . TEST NO. 1 COMPRESSION - SIDE 1
TEST NO. 5 COMPRESSION - SIDE 1

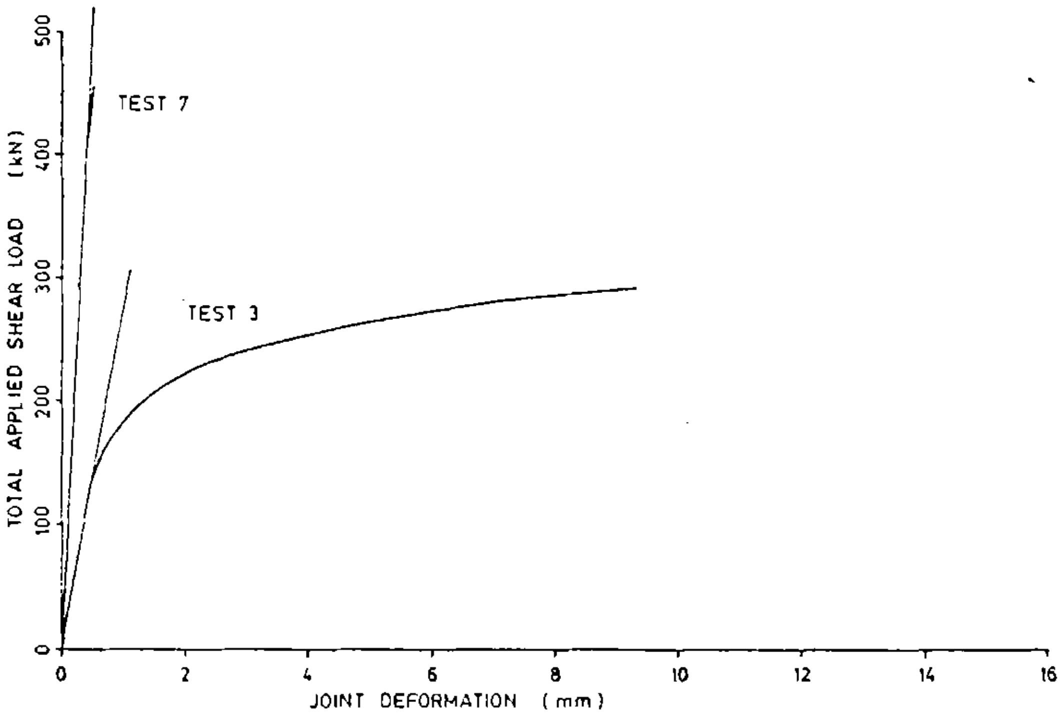

FIGURE 17f . TEST NO. 3 COMPRESSION - SIDE 2
TEST NO. 7 COMPRESSION - SIDE 1

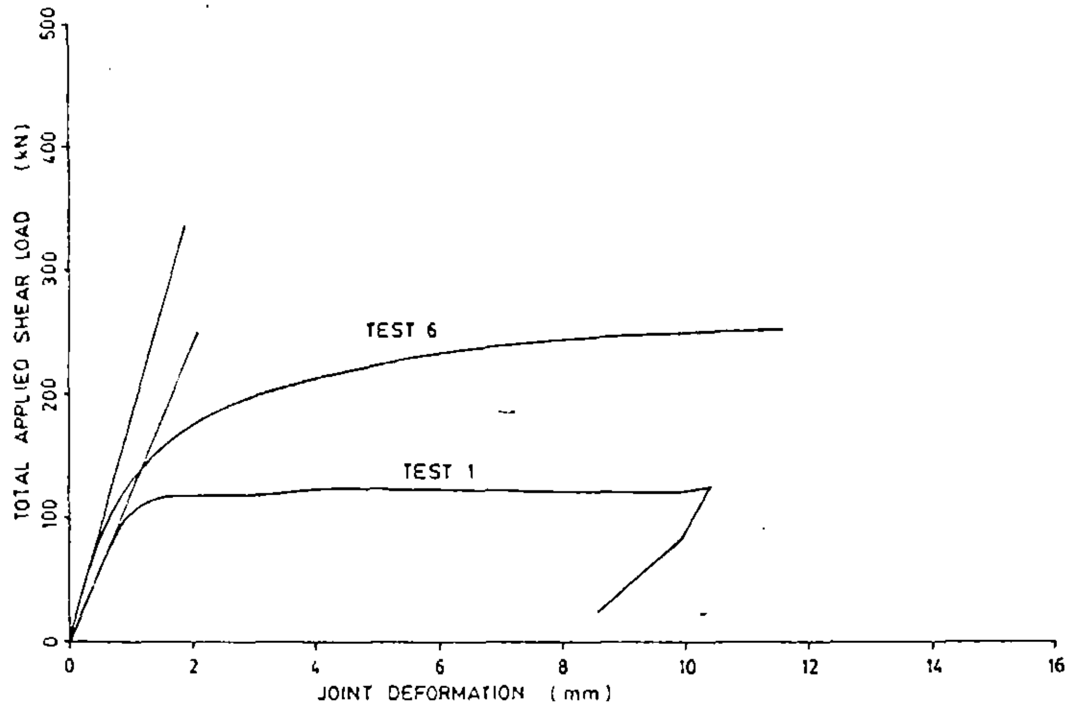

FIGURE 17g. TEST NO.1 COMPRESSION - SIDE 1
TEST NO.6 COMPRESSION - SIDE 1

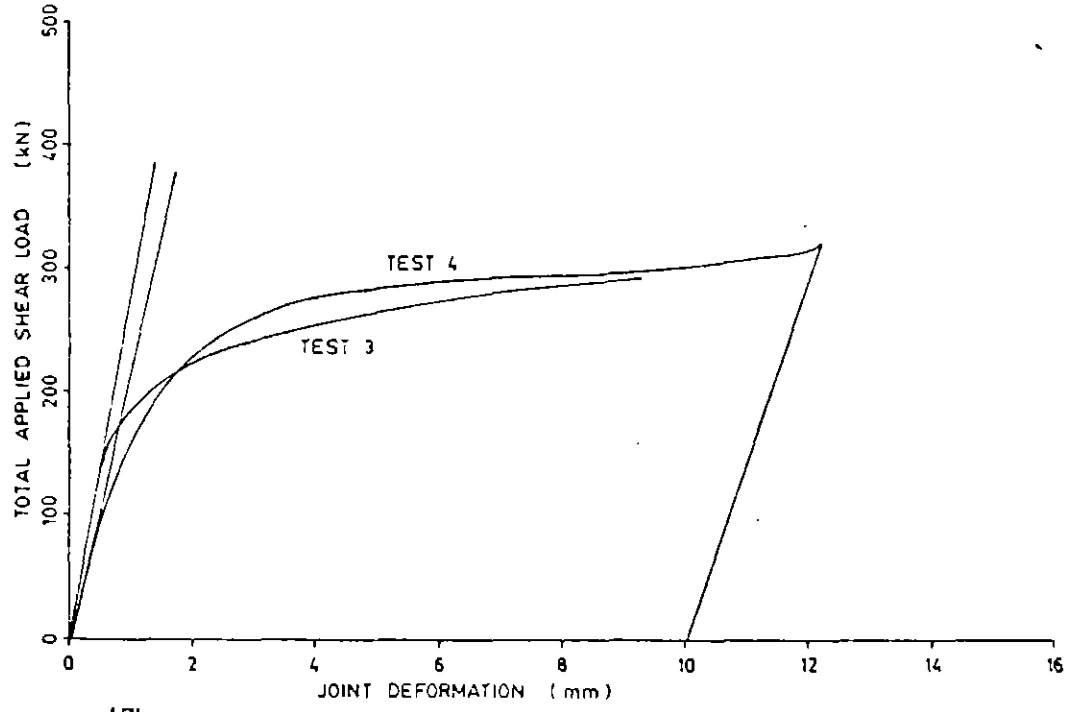

FIGURE 17h. TEST NO. 3 COMPRESSION - SIDE 2
TEST NO. 4 COMPRESSION - SIDE 1

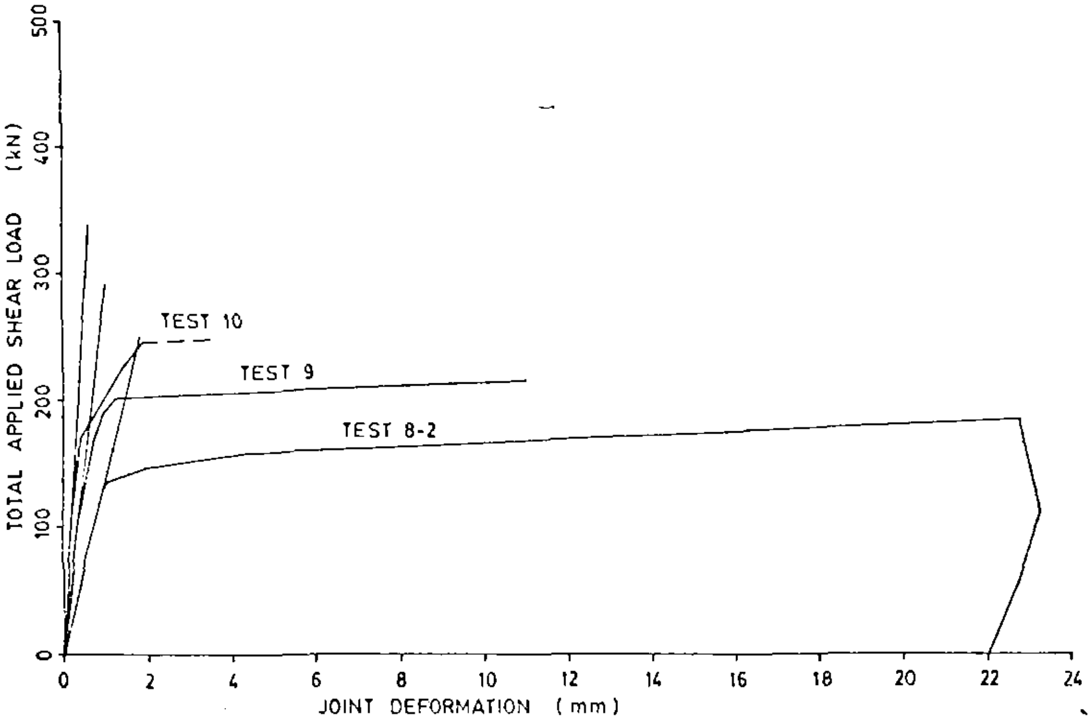

FIGURE 17i . TEST NO.8-2 COMPRESSION - SIDE 1
TEST NO. 9 COMPRESSION - SIDE 1
TEST NO. 10 COMPRESSION - SIDE 1

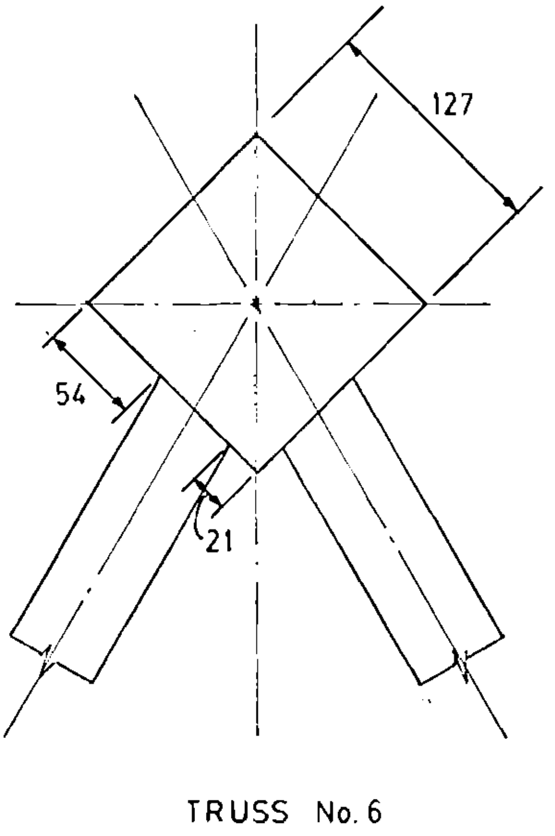

Fig. 18. Joint geometry for 60° trusses